BAW-2125

December 1990

ANALYSIS OF CAPSULE TE1-D
THE TOLEDO EDISON COMPANY
DAVIS BESSE NUCLEAR POWER STATION UNIT 1

-- Reactor Vessel Material Surveillance Program --

B&W NUCLEAR SERVICE COMPANY

BAW-2125

December 1990

ANALYSIS OF CAPSULE TE1-D
THE TOLEDO EDISON COMPANY
DAVIS BESSE NUCLEAR POWER STATION UNIT 1

-- Reactor Vessel Material Surveillance Program --

B&W NUCLEAR SERVICE COMPANY

BAW-2125

December 1990

ANALYSIS OF CAPSULE TE1-D
THE TOLEDO EDISON COMPANY
DAVIS BESSE NUCLEAR POWER STATION UNIT 1

-- Reactor Vessel Material Surveillance Program --

by

A. L. Lowe, Jr., PE
J. D. Aadland
J. W. Moore, III
L. Petrusha
W. R. Stagg

B&W Document No. 77-2125-00
B&W Contract No. 579-7735
(See Section 11 for document signatures)

B&W Nuclear Service Company
Engineering and Plant Services Division
P. O. Box 10935
Lynchburg, Virginia 24506-0935

B&W NUCLEAR SERVICE COMPANY

SUMMARY

This report describes the results of the examination of the fourth capsule of the Toledo Edison Company's Davis Besse Nuclear Power Station Unit 1 reactor vessel surveillance program. The capsule was removed and examined at the end of the sixth fuel cycle. The objective of the program is to monitor the effects of neutron irradiation on the tensile and fracture toughness properties of the reactor vessel materials by the testing and evaluation of tension, Charpy impact, and compact fracture toughness specimens. The program was designed in accordance with the requirements of Appendix H to 10CFR50 and ASTM Specification E185-73. The capsule received an average fast fluence of 9.62×10^{18} n/cm^2 (E > 1.0 Mev) and the predicted fast fluence for the reactor vessel T/4 location at the end of the sixth cycle is 1.36×10^{18} n/cm^2 (E > 1 MeV). Based on the calculated fast flux at the vessel wall, an 80% capacity factor, and the planned fuel management, the projected fast fluence that the Davis Besse Unit 1 reactor pressure vessel inside surface will receive in 40 calendar years of operation is 1.11×10^{19} n/cm^2 (E > 1 MeV).

The results of the tension tests indicated that the materials exhibited normal behavior relative to neutron fluence exposure. The Charpy impact data results exhibited the characteristic behavior of shift to higher temperature for the 30 ft-lb transition temperature as a result of neutron fluence damage and a decrease in upper shelf energy. These results showed that the current techniques used for predicting the change in both the increase in the RT_{NDT} and the decrease in upper shelf properties due to irradiation are conservative. The recommended operating period was extended to 32 effective full power years. These new operating limitations are in accordance with the requirements of Appendix G of 10CFR50.

CONTENTS

Contents (Cont'd)

List of Tables

Tables (Cont'd)

List of Figures

Figures (Cont'd)

1. INTRODUCTION

This report describes the results of the examination of the fourth capsule of the Toledo Edison Company's Davis Besse Nuclear Power Station Unit 1 reactor vessel material surveillance program. The capsule was removed and examined at the end of the sixth fuel cycle (5.45 EFPY). The first capsule of the program was removed and evaluated after the first year of operation; the results are reported in BAW-1701.[1] The second capsule of the program was removed and evaluated after the third fuel cycle (2.58 EFPY); the results are reported in BAW-1834.[2] The third capsule was removed and evaluated after the fourth fuel cycle (3.33 EFPY); the results are reported in BAW-1882.[3]

The objective of the program is to monitor the effects of neutron irradiation on the tensile and impact properties of reactor pressure vessel materials under actual operating conditions. The surveillance program for Davis Besse Unit 1 was designed and furnished by Babcock & Wilcox (B&W) as described in BAW-10100A.[4] The program, designed in accordance with the requirements of 10CFR50, Appendix H[5] and ASTM Specification E185-73[6], is being conducted in accordance with BAW-1543[7] and ASTM specification E185-82[8] and was planned to monitor the effects of neutron irradiation on the reactor vessel materials for the 40-year design life, i.e., 32 effective full power years (EFPY), of the reactor pressure vessel. The future operating limitations established after the evaluation of the surveillance capsule are also in accordance with the requirements of 10CFR50, Appendixes G[9] and H[5]. The recommended operating period was extended to 32 EFPY as a result of the fourth capsule evaluation.

2. BACKGROUND

The ability of the reactor pressure vessel to resist fracture is the primary factor in ensuring the safety of the primary system in light water-cooled reactors. The beltline region of the reactor vessel is the most critical region of the vessel because it is exposed to neutron irradiation. The general effects of fast neutron irradiation on the mechanical properties of such low-alloy ferritic steels as SA508, Class 2, used in the fabrication of the Davis Besse Unit 1 reactor vessel, are well characterized and documented in the literature. The low-alloy ferritic steels used in the beltline region of reactor vessels exhibit an increase in ultimate and yield strength properties with a corresponding decrease in ductility after irradiation. The most significant mechanical property change in reactor pressure vessel steels is the increase in temperature for the transition from brittle to ductile fracture accompanied by a reduction in the Charpy upper shelf impact toughness.

Appendix G to 10CFR50, "Fracture Toughness Requirements," specifies minimum fracture toughness requirements for the ferritic materials of the pressure-retaining components of the reactor coolant pressure boundary (RCPB) of water-cooled power reactors, and provides specific guidelines for determining the pressure-temperature limitations on operation of the RCPB. The toughness and operational requirements are specified to provide adequate safety margins during any condition of normal operation, including anticipated operational occurrences and system hydrostatic tests, to which the pressure boundary may be subjected over its service lifetime. Although the requirements of Appendix G to 10CFR50 became effective on August 13, 1973, the requirements are applicable to all boiling and pressurized water-cooled nuclear power reactors, including those under construction or in operation on the effective date.

Appendix H to 10CFR50, "Reactor Vessel Materials Surveillance Program Requirements," defines the material surveillance program required to monitor changes in the fracture toughness properties of ferritic materials in the reactor vessel beltline region of water-cooled reactors resulting from exposure to neutron irradiation and the thermal environment. Fracture toughness test data are obtained from material specimens withdrawn periodically from the reactor vessel. These data will permit determination of the conditions under which the vessel can be operated with adequate safety margins against fracture throughout its service life.

A method for guarding against brittle fracture in reactor pressure vessels is described in Appendix G to the ASME Boiler and Pressure Vessel Code, Section III, "Nuclear Power Plant Components." This method utilizes fracture mechanics concepts and the reference nil-ductility temperature, RT_{NDT}, which is defined as the greater of the drop weight nil-ductility transition temperature (per ASTM E-208) or the temperature that is 60F below that at which the material exhibits 50 ft-lbs and 35 mils lateral expansion. The RT_{NDT} of a given material is used to index that material to a reference stress intensity factor curve (K_{IR} curve), which appears in Appendix G of ASME Section III. The K_{IR} curve is a lower bound of dynamic, static, and crack arrest fracture toughness results obtained from several heats of pressure vessel steel. When a given material is indexed to the K_{IR} curve, allowable stress intensity factors can be obtained for this material as a function of temperature. Allowable operating limits can then be determined using these allowable stress intensity factors.

The RT_{NDT} and, in turn, the operating limits of a nuclear power plant, can be adjusted to account for the effects of radiation on the properties of the reactor vessel materials. The radiation embrittlement and the resultant changes in mechanical properties of a given pressure vessel steel can be monitored by a surveillance program in which a surveillance capsule containing prepared specimens of the reactor vessel materials is periodically removed from the operating nuclear reactor and the specimens are tested. The increase in the Charpy V-notch 30 ft-lb temperature is added to the original RT_{NDT} to adjust it

for radiation embrittlement. This adjusted RT_{NDT} is used to index the material to the K_{IR} curve which, in turn, is used to set operating limits for the nuclear power plant. These new limits take into account the effects of irradiation on the reactor vessel materials.

3. SURVEILLANCE PROGRAM DESCRIPTION

The surveillance program comprises six surveillance capsules designed to monitor the effects of neutron and thermal environment on the materials of the reactor pressure vessel core region. The capsules, which were inserted into the reactor vessel before initial plant startup, were positioned inside the reactor vessel between the thermal shield and the vessel wall at the locations shown in Figure 3-1. The six capsules, originally designed to be placed two in each holder tube, are positioned near the peak axial and azimuthal neutron flux. However, with the use of Davis Besse Unit 1 as one of the irradiation sites of the 177-fuel-assembly integrated reactor vessel material surveillance program, the capsules are irradiated on a schedule integrated with the capsules of the other participating reactors. This integrated schedule is described in BAW-1543. BAW-10100A includes a full description of the capsule design.

Capsule TE1-D was removed during the sixth refueling shutdown of Davis Besse Unit 1. This capsule contained Charpy V-notch impact test specimens fabricated from one base metal (SA508, Class 2), a weld metal, and heat-affected-zone material. Tensile specimens were fabricated from one base metal and the weld metal only. In addition, there are compact fracture specimens fabricated from the weld metal. The specimens contained in the capsule are described in Table 3-1, and the location of the individual specimens within the capsule are described in Figure 3-2. The chemical composition and heat treatment of the surveillance material in capsule TE1-D are described in Table 3-2.

All test specimens were machined from the 1/4-thickness (1/4T) location of the forging material. Charpy V-notch and tension test specimens from the vessel material were oriented with their longitudinal axes perpendicular to the

principal working direction of the forging. Capsule TE1-D contained dosimeter wires, described as follows:

Dosimeter Wire	Shielding
U-Al alloy	Cd-Ag alloy
Np-Al alloy	Cd-Ag alloy
Nickel	Cd-Ag alloy
0.66 wt % Co-Al alloy	Cd-Ag alloy
0.66 wt % Co-Al alloy	None
Fe	None

Thermal monitors of low-melting metals and alloys were included in the capsule. The metals and alloys and their melting points are as follows:

Alloy	Melting Point, F
90% Pb, 5% Ag, 5% Sn	558
97.5% Pb, 2.5% Ag	580
97.5% Pb, 1.5% Ag, 1.0% Sn	588
Cadmium	610
Lead	621

Table 3-1. Specimens in Surveillance Capsule TE1-D

Material Description	Material Identity	No. of Test Specimens Tension	CVN Impact	1/2T CT
Weld Metal	WF-182-1	2	12	8
Weld, HAZ Heat SS, Transverse	BCC241	-	12	-
Base Metal Heat SS, Transverse	BCC241	2	12	-
Total Per Capsule		4	36	8

Table 3-2. Chemical Composition and Heat Treatment of Surveillance Materials

Chemical Analysis

Element	Heat BCC-241[a]	Weld Metal WF-182-1[b]
C	0.22	0.09
Mn	0.63	1.70
P	0.011	0.014
S	0.011	0.013
Si	0.27	0.42
Ni	0.81	0.63
Cr	0.32	0.15
Mo	0.63	0.40
Cu	0.02	0.21

Heat Treatment

Heat No.	Temp, F	Time, h	Cooling
BCC241	1640±10	4	Water quenched
	1590±10	4	Water quenched
	1240±10	5	Air cooled
	1125±25	15-1/2	Furnace cooled
WF-182-1	1125±25	15-1/2	Furnace cooled

[a] PerCertified Materials Test Reports

[b] PerLicensing Document BAW-1500[10]

Figure 3-1. Reactor Vessel Cross Section Showing Location of Capsule TE1-D in Davis Besse Unit 1

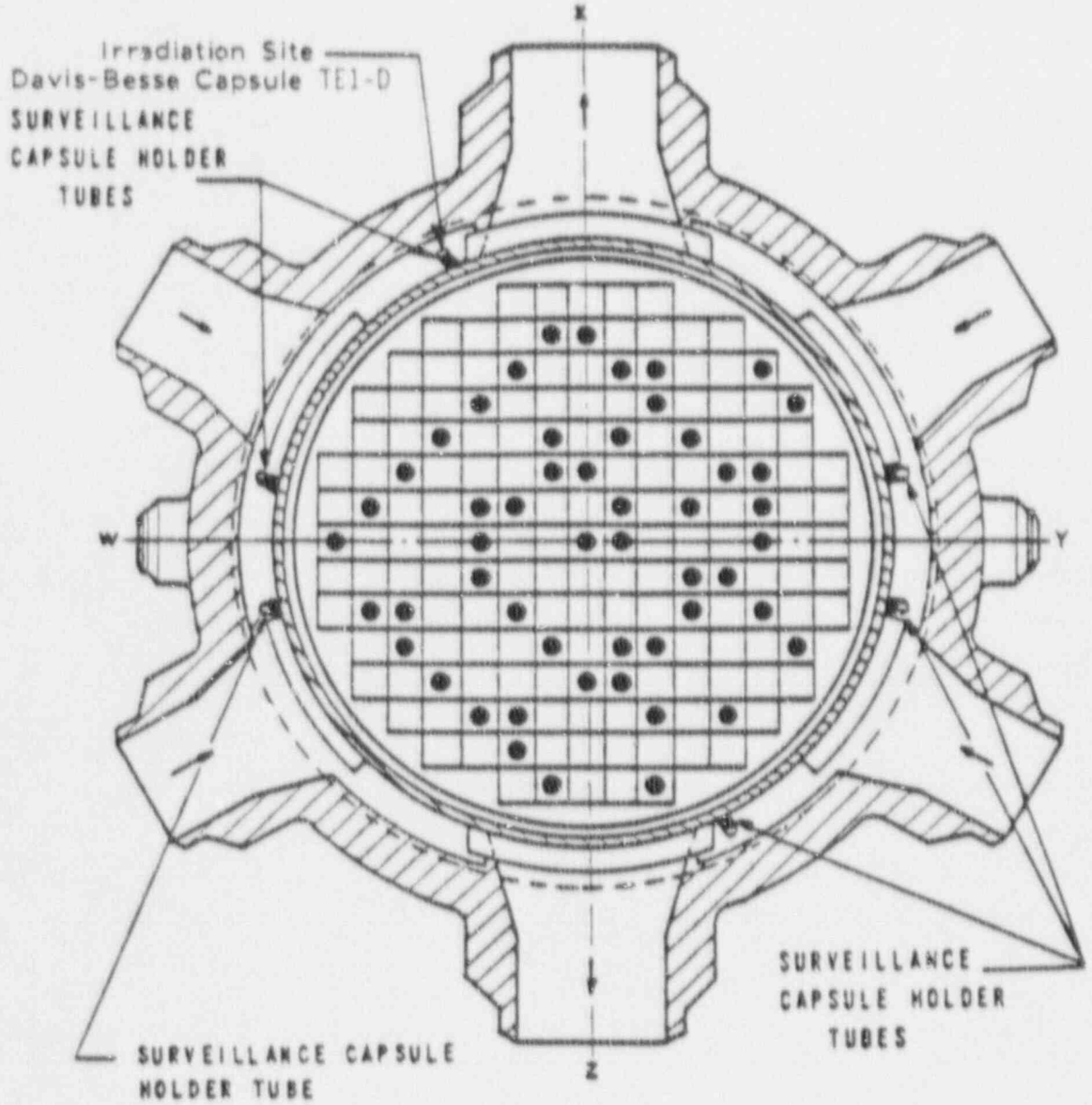

Figure 3-2. Loading Diagram for Test Specimens in TEI-D

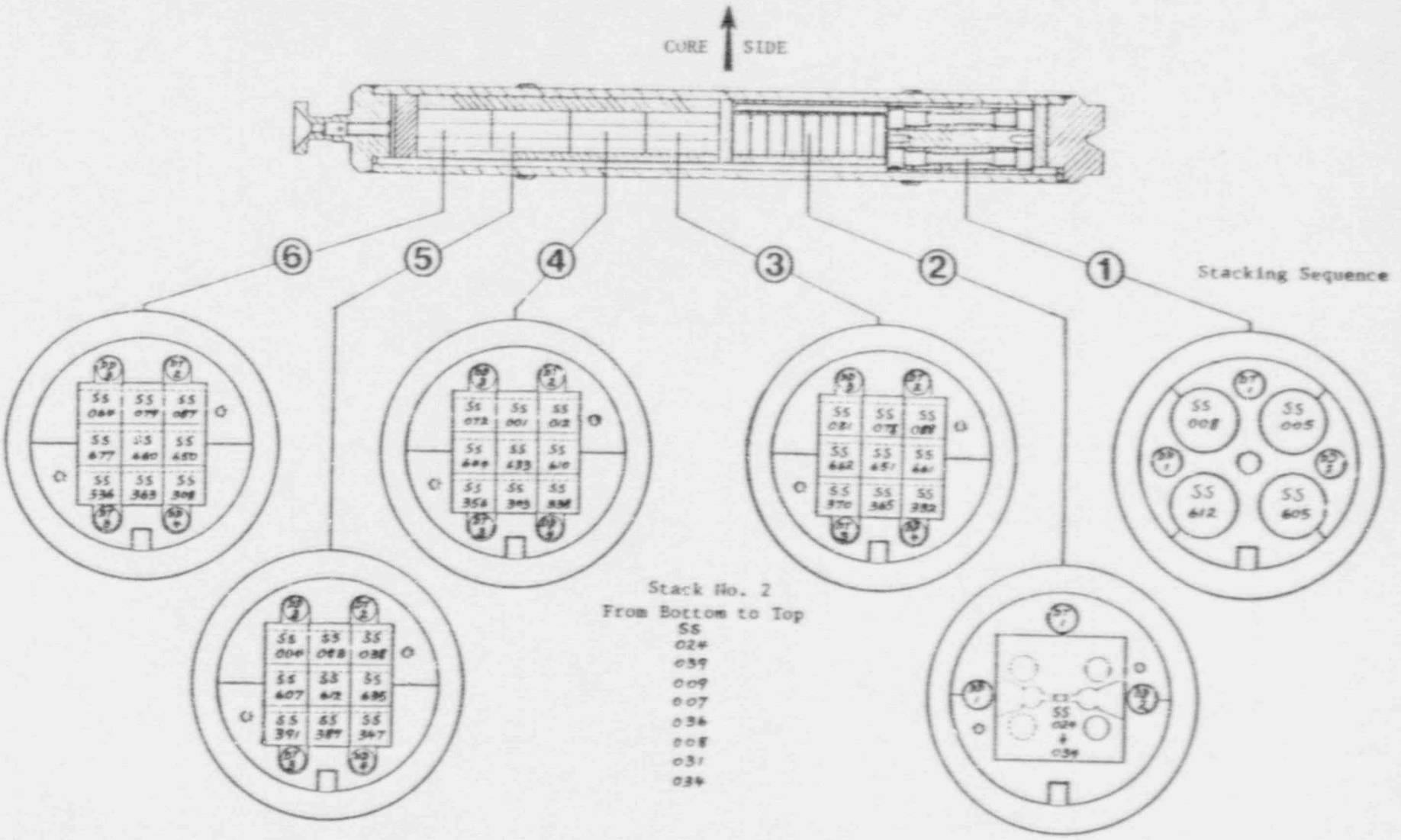

Loading Diagram for Test Specimens in Lower Surveillance Capsule TEI-D

4. PRE-IRRADIATION TESTS

Unirradiated material was evaluated for two purposes: (1) to establish a baseline of data to which irradiated properties data could be referenced, and (2) to determine those materials properties to the extent practical from available material, as required for compliance with Appendixes G and H to 10CFR50.

4.1. Tension Tests

Tension test specimens were fabricated from the reactor vessel shell course forging and weld metal. The subsize specimens were 4.25 inches long with a reduced section 1.750 inches long by 0.357 inch in diameter. They were tested on a 55,000-lb load capacity universal test machine at a crosshead speed of 0.050 inch per minute. A 4-pole extension device with a strain gaged extensometer was used to determine the 0.2% yield point. Test conditions were in accordance with the applicable requirements of ASTM A370-72.[11] For each material type and/or condition, six specimens in groups of three were tested at both room temperature and 580F. The tension-compression load cell used had a certified accuracy of better than $\pm$0.5% of full scale (25,000 lb). All test data for the pre-irradiation tensile specimens are given in Appendix B.

4.2. Impact Tests

Charpy V-notch impact tests were conducted in accordance with the requirements of ASTM Standard Methods A370-72 and E23-72[12] on an impact tester certified to meet Watertown standards. Test specimens were of the Charpy V-notch type, which were nominally 0.394 inch square and 2.165 inches long.

Prior to testing, specimens were temperature-controlled in liquid immersion baths, capable of covering the temperature range from -85 to +550F. Specimens

were removed from the baths and positioned in the test frame anvil with tongs specifically designed for the purpose. The pendulum was released manually, allowing the specimens to be broken within 5 seconds from their removal from the temperature baths.

Impact test data for the unirradiated baseline reference materials are presented in Appendix C. Tables C-1 through C-3 contain the basis data that are plotted in Figures C-1 through C-3.

5. POST-IRRADIATION TESTS

5.1. Thermal Monitors

Capsule TE1-D contained three temperature monitor holder tubes, each containing five fusible alloy wires with melting points ranging from 558 to 621F. All the thermal monitors at 558, 580, and 588F had melted while those at the 610F location showed no signs of melting of slumping; the monitor at the 621F location melted in all three holder tubes. It was heretofore assumed that the 610F and 621F monitors were placed in the wrong locations in the holder tubes, and based on these observations, it was concluded that the capsule had been exposed to a peak temperature in the range of 610 to 621F during the reactor operating period.

In the case of TE1-D the original loading diagram was consulted. This drawing lists the five materials used in the monitors, and showed the position in which each wire was loaded. Both show the lead wire (621F melting point) to be in the fourth position, with the cadmium wire (610F melting point) in the fifth position.

This supports the observation that the 610F monitor did not melt while the 621F monitor did melt. It is believed that the lead wire softened (and presented the appearance of melting) due to long term exposure to elevated temperatures, which were not sufficient to melt the cadmium wire. Therefore, it is probable that the capsules was exposed to temperatures in excess of 588F but not as high as 610F, and that this was sufficient to cause the lead wires to slump and appear to have melted.

These peak temperatures are attributed to operating transients that are of short durations as described in BAW-2040[13] and are judged to have insignificant effect on irradiation damage. Short duration operating transients cause the use of

thermal monitor wires to be of limited value in determining the maximum steady state operating temperature of the surveillance capsules; however, it was calculated that the maximum steady state operating temperature of specimens in the capsule was held within +25F of the 1/4T vessel thickness location temperature of 561 as described in BAW-2040. It is concluded that the capsule design temperature may have been exceeded during operating transients but not for times and temperatures that would make the capsule data unusable.

5.2. Tension Test Results

The results of the postirradiation tension tests are presented in Table 5-1. Tests were performed on specimens at both room temperature and 550 using the same test procedures and techniques used to test the unirradiated specimens (Section 4.1). In general, the ultimate strength and yield strength of the material increased with a corresponding slight decrease in ductility; both effects were the result of neutron radiation damage. The type of behavior observed and the degree to which the material properties changed is within the range of changes to be expected for the radiation environment to which the specimens were exposed.

The results of the pre-irradiation tension tests are presented in Appendix B.

5.3. Charpy V-Notch Impact Test Results

The test results from the irradiated Charpy V-notch specimens of the reactor vessel beltline material are presented in Tables 5-2 through 5-4 and Figures 5-1 through 5-3. The test procedures and techniques were the same as those used to test the unirradiated specimens (Section 4.2). The data show that the materials exhibited a sensitivity to irradiation within the values to be expected from their chemical composition and the fluence to which they were exposed.

Scatter in the heat-affected zone material normally prevents a serious interpretation of the data. Although the data contained in this capsule results appear to follow a smooth trend, the data at 550F is significantly below the upper-shelf trend and, therefore, must be classified as abnormal scatter.

The results of the pre-irradiation Charpy V-notch impact tests are given in Appendix C.

5.4. Compact Fracture Toughness Tests

The compact fracture toughness specimens fabricated from the weld metal, which were a part of the capsule specimen inventory, were tested by a recognized single specimen J-integral testing procedure. The results of the testing of these specimens is reported in a separate report, BAW-2128.[14]

Table 5-1. Tensile Properties of Capsule TE1-D Irradiated Base Metal and Weld Metal

Specimen No.	Test Temp, F	Strength, psi		Elongation, %		Red'n. in Area, %
		Yield	Ultimate	Uniform	Total	
Base Metal, Transverse, 9.62×10^{18} n/cm^2 (E > 1 MeV)						
SS-612	70	73,800	95,200	10	25	61
SS-605	550	69,500	91,900	9	22	58
Weld Metal, 9.62×10^{18} n/cm^2 (E > 1 MeV)						
SS-008	70	87,300	103,300	10	25	56
SS-005	550	78,100	94,800	9	18	48

Table 5-2. Charpy Impact Data for Capsule TE1-D Base Metal, Heat BCC241, Irradiated to 9.62×10^{18} n/cm^2 (E > 1 MeV)

Specimen No.	Test Temp., F	Absorbed Energy, ft-lb	Lateral Expansion, 10^{-3} in.	Shear Fracture, %
SS 651	0	23.5	15	10
SS 610	15	14.0	13	10
SS 660	15	44.0	34	10
SS 607	25	41.0	29	10
SS 662	40	51.0	42	20
SS 661	70	48.0	39	30
SS 612	125	86.0	70	50
SS 635	200	117.0*	82	100
SS 644	250	120.0*	88	100
SS 633	350	113.5*	84	100
SS 650	450	111.0	83	100
SS 677	550	103.5	87	100

*Values used to determine upper-shelf energy value per ASTM E185.

Table 5-3. Charpy Impact Data for Capsule TE1-D Heat-Affected Zone Metal, Heat BCC241, Irradiated to 9.62×10^{18} n/cm^2 (E > 1 MeV)

Specimen No.	Test Temp., F	Absorbed Energy, ft-lb	Lateral Expansion, 10^{-3} in.	Shear Fracture, %
SS 391	-50	29.0	11	10
SS 347	-25	28.5	17	20
SS 363	0	30.0	18	10
SS 308	5	34.0	23	20
SS 332	10	50.0	41	40
SS 303	25	72.5	51	70
SS 365	70	91.5	65	70
SS 336	125	98.5	75	95
SS 356	200	119.5*	78	100
SS 389	250	115.0*	85	100
SS 370	350	115.0*	80	100
SS 338	550	77.0	70	100

*Values used to determine upper-shelf energy value per ASTM E185.

Table 5-4. Irradiated Charpy Impact Data for Capsule TE1-D Weld Metal Irradiated to 9.62 x 10^{18} n/cm^2 (E > 1 MeV)

Specimen No.	Test Temp., F	Absorbed Energy, ft-lb	Lateral Expansion, 10^{-3} in.	Shear Fracture, %
SS 001	70	14.0	14	10
SS 038	125	26.5	27	30
SS 004	140	32.5	28	50
SS 088	160	33.0	29	50
SS 072	175	40.0	38	50
SS 031	200	48.5	44	70
SS 087	250	53.5*	49	100
SS 083	300	49.0*	48	100
SS 078	350	60.0*	56	100
SS 012	400	54.0*	49	100
SS 079	550	52.5	55	100

*Values used to determine upper-shelf energy value per ASTM E185.

Figure 5-1. Impact Data for Irradiated Shell Forging Material, Heat BCC-241

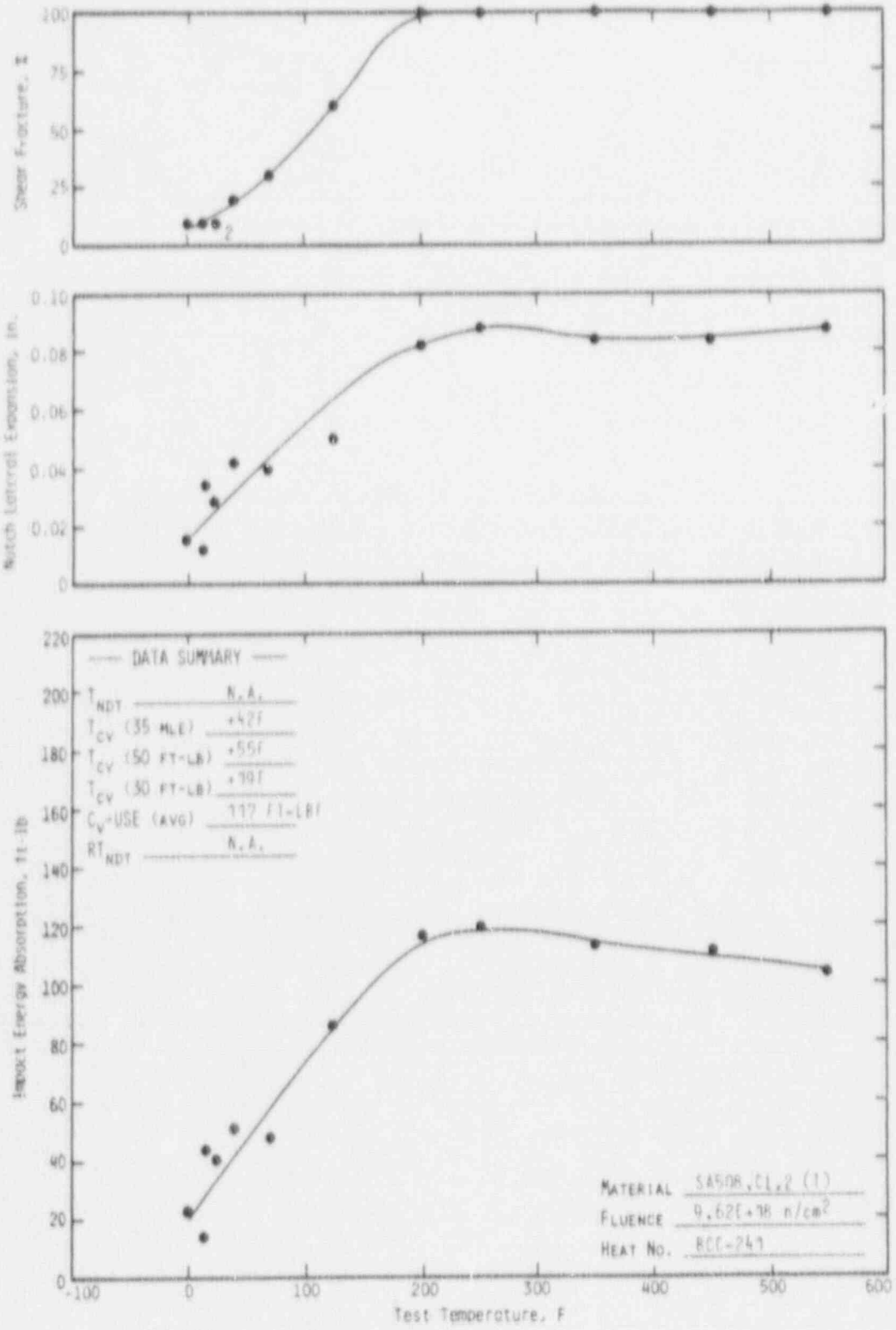

Figure 5-2. Impact Data for Irradiated Shell Forging Material, Heat-Affected Zone, Heat BCC-241

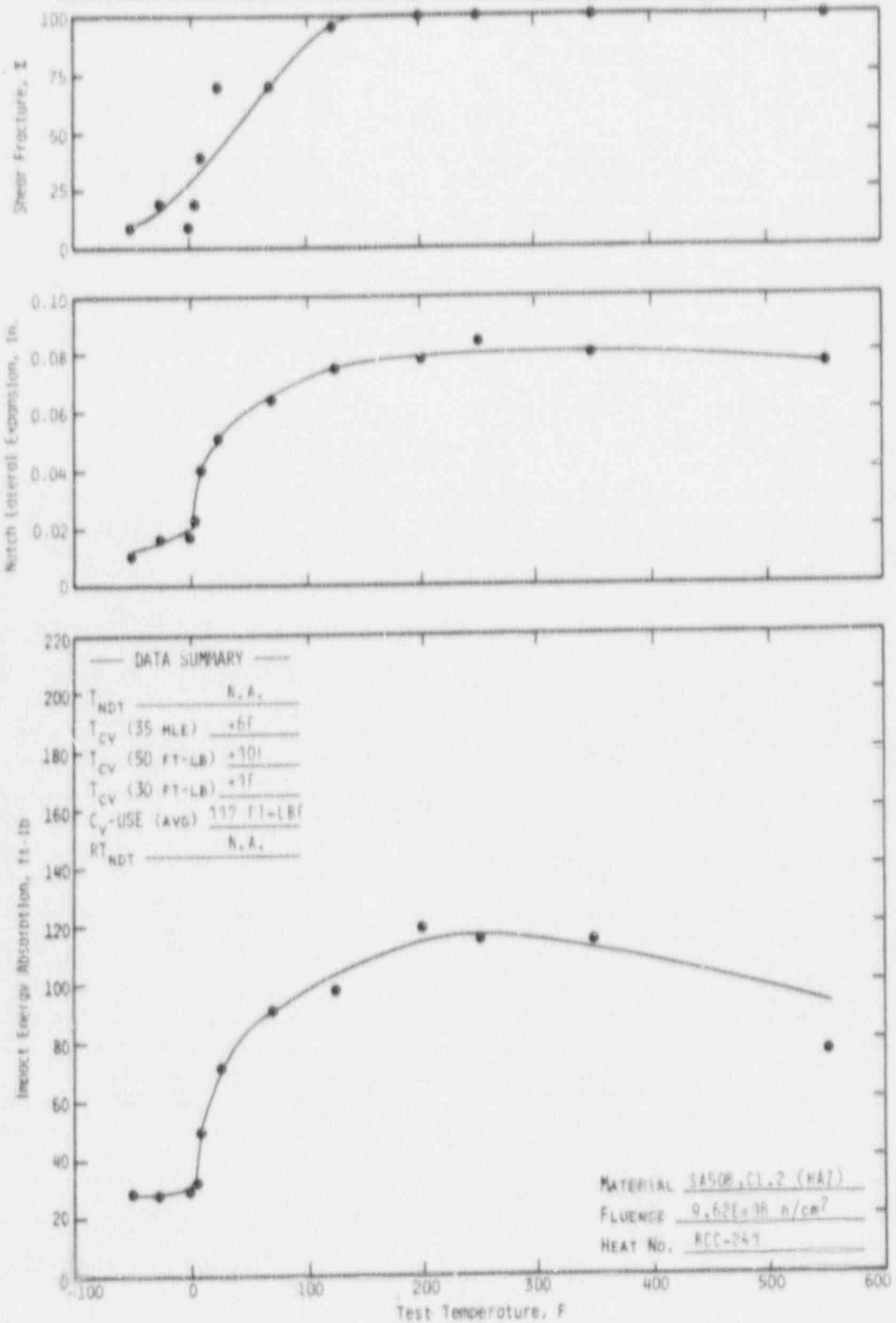

Figure 5-3. Impact Data for Irradiated Weld Metal, WF-182-1

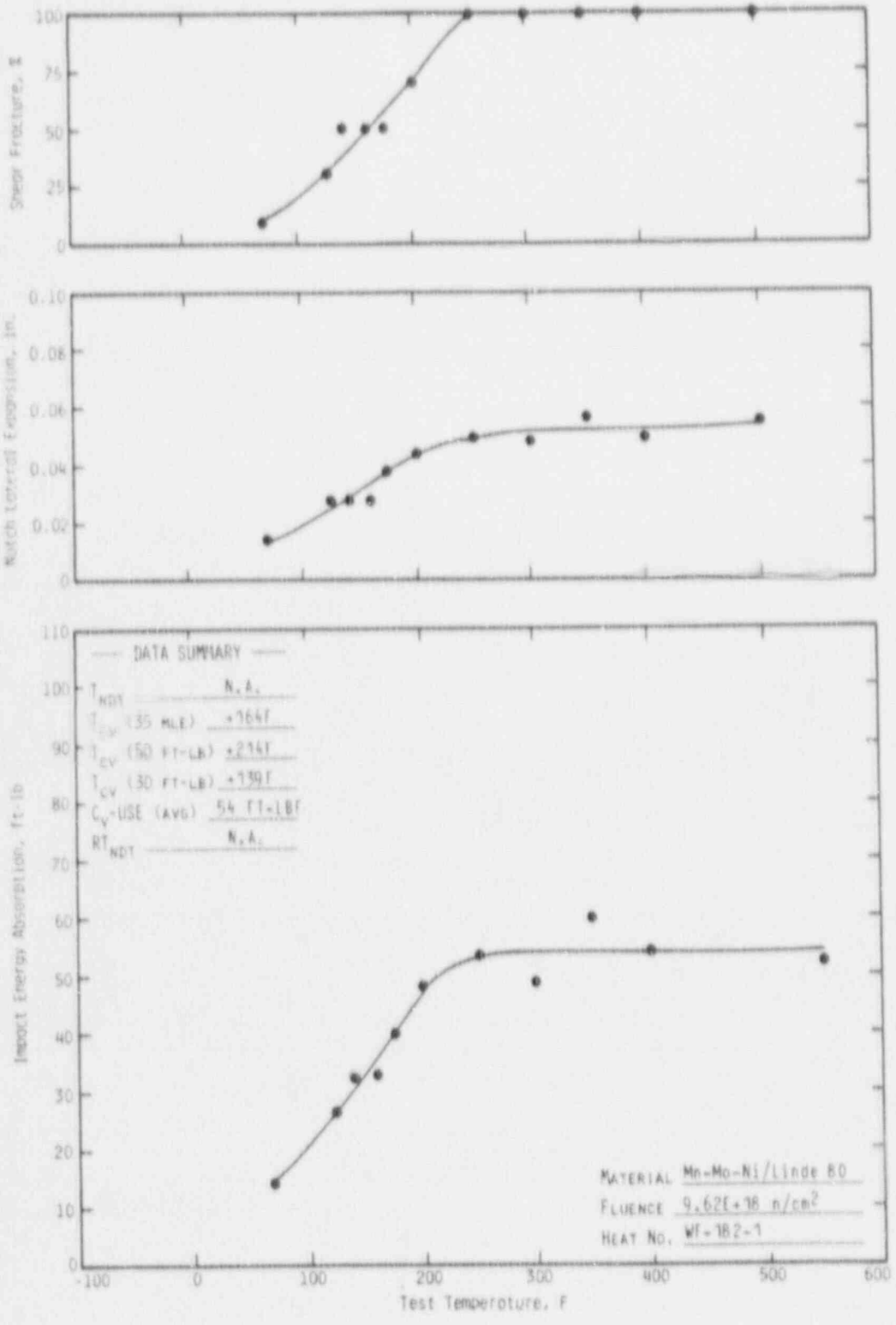

6. NEUTRON FLUENCE

6.1. Introduction

The neutron fluence (time integral of flux) is a quantative way of expressing the cumulative exposure of a material to a pervading neutron flux over a specific period of time. Fast neutron fluence, defined as the fluence of neutrons having energies greater than 1 MeV, is the parameter that is presently used to correlate radiation induced changes in material properties. Accordingly, the fast fluence must be determined at two locations: (1) in the test specimens located in the surveillance capsule, and (2) in the wall of the reactor vessel. The former is used in developing the correlation between fast fluence and changes in the material properties of specimens, and the latter is used to ascertain the point of maximum fluence in the reactor vessel, the relative radial and azimuthal distribution of the fluence, the fluence gradient through the reactor vessel wall, and the corresponding material properties.

The accurate determination of neutron flux is best accomplished through the simultaneous consideration of neutron dosimeter measurements and analytically derived flux spectra. Dosimeter measurements alone cannot be used to predict the fast fluence in the vessel wall or in the test specimens because (1) they cannot measure the fluence at the points of interest, and (2) they provide only rudimentary information about the neutron energy spectrum. Conversely, reliance on calculations alone to predict fast fluence is not prudent because of the length and complexity of the analytical procedures involved. In short, measurements and calculations are necessary complements of each other and together they provide assurance of accurate results.

Therefore, the determination of the fluence is accomplished using a combined analytical-empirical methodology which is outlined in Figure 6-1 and described in the following paragraphs. The details of the procedures and methods are presented in general terms in Appendix D and in BAW-1485P.[15]

Figure 6-1. General Fluence Determination Methodology

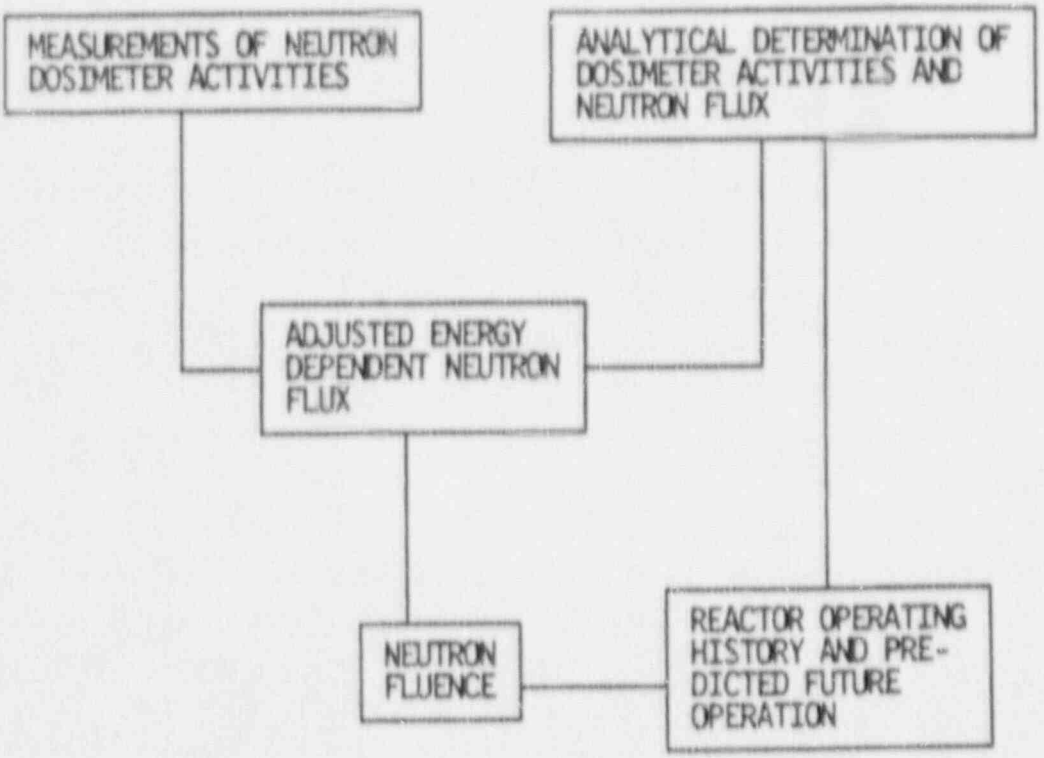

Analytical Determination of Dosimeter Activities and Neutron Flux

The analytical calculation of the space and energy dependent neutron flux in the test specimens and in the reactor vessel is performed with the two dimensional discrete ordinates transport code, DOTIV.[16] The calculations employ an angular quadrature of 48 sectors (S8), a third order LeGendre polynomial scattering approximation (P3), the CASK23E cross section set[17] with 22 neutron energy groups and a fixed distributed source corresponding to the time weighted average power distribution for the applicable irradiation period.

In addition to the flux in the test specimens, the DOTIV calculation determines the saturated specific activity of the various neutron dosimeters located in the surveillance capsule using the ENDF/B5 dosimeter reaction cross sections.[18] The saturated activity of each dosimeter is then adjusted by a factor which corrects

for the fraction of saturation attained during the dosimeter's actual (finite) irradiation history. Additional corrections are made to account for the following effects:

- Photon induced fissions in U and Np dosimeters (without this correction the results underestimate the measured activity).
- Fissile impurities in U dosimeters (without this correction the results underestimate the measured activity).
- Short half-life of isotopes produced in iron and nickel dosimeters (303-day Mn-54 and 71-day Co-58, respectively). (Without this correction, the results could be biased high or low depending on the long term versus short term power histories.)

Measurement of Neutron Dosimeter Activities

The accuracy of neutron fluence predictions is improved if the calculated neutron flux is compared with neutron dosimeter measurements adjusted for the effects noted above. The neutron dosimeters located in the surveillance capsules are listed in Table 6-1. Both activation type and fission type dosimeters were used.

The ratio of measured dosimeter activity to calculated dosimeter activity (M/C) is determined for each dosimeter, as discussed in Appendix D. These M/C ratios are evaluated on a case-by-case basis to assess the dependability or veracity of each individual dosimeter response. After carefully evaluating all factors known to affect the calculations or the measurements, an average M/C ratio is calculated and defined as the "normalization factor." The normalization factor is applied as an adjustment factor to the DOT-calculated flux at all points of interest.

Neutron Fluence

The determination of the neutron fluence from the time averaged flux requires only a simple multiplication by the time in EFPS (effective full-power seconds) over which the flux was averaged, i.e.

$$f_{ij}(\Delta T) = \sum_{g} \phi_{ijg} \Delta T$$

where

$f_{ij}(\Delta T)$ = Fluence at (i,j) accumulated over time ΔT (n/cm^2),

g = Energy group index,

ϕ_{ijg} = Time-average flux at (i,j) in energy group g, (n/cm^2-sec),

ΔT = Irradiation time, EFPS.

Neutron fluence was calculated in this analysis for the following components over the indicated operating time:

Test Specimens: Capsule irradiation time in EFPS

Reactor Vessel: Vessel irradiation time in EFPS

Reactor Vessel: Maximum point on inside surface extrapolated to 32 effective full power years

The neutron exposure to the reactor vessel and the material surveillance specimens was also determined in terms of the iron atom displacements per atom of iron (DPA). The iron DPA is an exposure index giving the fraction of iron atoms in an iron specimen which would be displaced during an irradiation. It is considered to be an appropriate damage exposure index since displacements of atoms from their normal lattice sites is a primary source of neutron radiation damage. DPA was calculated based on the ASTM Standard E693-79 (reapproved 1985).[19] A DPA cross section for iron is given in the ASTM Standard in 641 energy groups. DPA per second is determined by multiplying the cross section at a given energy by the neutron flux at that energy and integrating over energy. DPA is then the integral of DPA per second over the time of the irradiation. In the DPA calculations reported herein, the ASTM DPA cross sections were first collapsed to the 22 neutron group structure of CASK-23E; the DPA was then determined by summing the group flux times the DPA cross section over the 22 energy groups and multiplying by the time of the irradiation.

6.2. Vessel Fluence

The maximum fluence (E > 1 MeV) exposure of the Davis Besse Unit 1 reactor vessel during Cycles 1-6 was determined to be 2.44 x 10^{18} n/cm^2 based on a maximum neutron flux of 1.42 x 10^{10} n/cm^2-s (Tables 6-2 and 6-3). The maximum fluence occurs at the cladding/vessel interface at an azimuthal location of approximately 11 degrees from a major horizontal axis of the core.

Fluence data were extrapolated to 32 EFPY of operation based on two assumptions: (1) the future fuel cycle operations do not differ significantly from their current designs, and (2) the latest calculated (or extrapolated) flux remains constant from that time through 32 EFPY. The extrapolation was carried out in two stages, (1) from EOC-6 to EOC-7, and (2) from EOC-7 to 32 EFPY. In the first stage, Cycle 7 fuel design information is used to calculate assembly averaged relative power distributions. These power distributions are used with DOT adjoint factors to determine the average fast flux for Cycle 7. In the second stage, the 32 EFPY fluence was calculated by assuming a constant flux over the period which was equal to the average flux for cycle 7.

Relative fluence and DPA (displacement per atom) as a function of radial location in the reactor vessel wall is shown in Figure 6-2. Reactor vessel neutron fluence lead factors, which are the ratio of the neutron flux at the clad interface to that in the vessel wall at the T/4, T/2 and 3T/4 locations, are 1.79, 3.54, and 7.28, respectively. DPA lead factors at the same locations are 1.59, 2.64, and 4.57, respectively. The relative fluence as a function of azimuthal angle is shown in Figure 6-3. A peak occurs in the fast flux (E > 1 MeV) at about 11 degrees with a corresponding value of 1.42 x 10^{10} n/cm^2-s.

6.3. Capsule Fluence

The capsule was irradiated for 1989.8 EFPD in the top holder tube position during Cycles 1-6 of Davis Besse located 26.9° degrees off the major horizontal axis at about 202 cm from the vertical axis of the core. The cumulative fast fluence at the center of the surveillance capsule was calculated to be 9.62 x 10^{18} n/cm^2. This fluence value represents an average value for the center location of the

Charpy specimens in the capsule. It includes an axial peaking factor in the capsule of 1.14 and a normalization factor of 1.03.

6.4. Fluence Uncertainties

Uncertainties were estimated for the fluence values reported herein. The results are shown in Table 6-5 and are based on comparisons to benchmark experiments, when available; estimated and measured variations in input data; and on engineering judgement. The values in Table 6-5 represent best estimate values based on past experience with reactor vessel fluence analyses.

Table 6-1. Surveillance Capsule Dosimeters

Dosimeter Reactions[a]	Lower Energy Limit for Reaction, MeV	Isotope Half-Life
$^{54}Fe(n,p)^{54}Mn$	2.5	312.5 days
$^{58}Ni(n,p)^{58}Co$	2.3	70.85 days
$^{238}U(n,f)^{137}Cs$	1.1	30.03 years
$^{237}Np(n,f)^{137}Cs$	0.5	30.03 years

[a] Reaction activities measured for capsule flux evaluation.

Table 6-2. Davis Besse Unit 1 Reactor Vessel Fast Flux

Cycle	Fast Flux (E > 1 MeV), n/cm^2-s				Flux n/cm^2-s (E > 0.1 MeV)
	Inside Surface (Max Location)	T/4	T/2	3T/4	Inside Surface (Max Location)
Cycle 1 (374 EFPD)	1.61E+10	8.9E+9	4.4E+9	2.0E+9	3.4E+10
Cycles 2-6 (1615.8 EFPD)	1.38E+10	7.71E+9	3.90E+9	1.90E+9	2.88E+10
Cycle 7** (390 EFPD)	1.03E+10	0.58E+10*	0.29E+10*	1.41E+9*	
8 EFPY	1.03E+10	0.58E+10*	0.29E+10*	1.41E+9*	
15 EFPY	1.03E+10	0.58E+10*	0.29E+10*	1.41E+9*	
21 EFPY	1.03E+10	0.58E+10*	0.29E+10*	1.41E+9*	
32 EFPY	1.03E+10	0.58E+10*	0.29E+10*	1.41E+9*	

*Divide flux at inside surface by the appropriate lead factors on p. 6-8 to obtain these T/4, T/2, and 3T/4 fast flux values.

**Assumed cycle length of 390 EFPD for flux extrapolation for Cycle 7.

Table 6-3. Calculated Davis Besse Unit 1 Reactor Vessel Fluence

Cumulative Irradiation Time	Fast Fluence, n/cm^2 (E > 1 MeV) Inside Surface (Max Location)	T/4	T/2	3T/4
End of Cycle 1 (374 EFPD)	5.19E+17	2.9E+17	1.4E+17*	6.8E+16
End of Cycle 6 (1989.8 EFPD)	2.44E+18	1.36E+18	6.89E+17	3.35E+17
End of Cycle 7 (2379.8 EFPD)	2.79E+18	1.56E+18*	7.88E+17*	3.83E+17*
8 EFPY	3.27E+18	1.83E+18*	9.24E+17*	4.49E+17*
15 EFPY	5.55E+18	3.10E+18*	1.57E+18*	7.62E+17*
21 EFPY	7.50E+18	4.19E+18*	2.12E+18*	1.03E+18*
32 EFPY	1.11E+19	6.20E+18*	3.14E+18*	1.52E+18*
*Calculated using these lead factors	1.0	1.79	3.54	7.28
Conversion Factors				
Fluence (E > 1 MeV) to DPA	1.45E-21**	1.63E-21**	1.94E-21**	2.31E-21**

**Multiply fast fluence values (E > 1 MeV) in units of n/cm^2 by these factors to obtain the corresponding DPA values.

Table 6-4. Surveillance Capsule TE1-D Fluence, Flux, and DPA

Irradiation Time	Flux ($E > 1$ MeV), n/cm^2-s	Fluence, n/cm^2	DPA
DB1, Cycles 1-6 (1989.8 EFPD)	5.60E+10	9.62E+18	1.40E-2

Table 6-5. Estimated Fluence Uncertainty

Calculated Fluence	Estimated Uncertainty	Basis of Estimate
In the capsule	± 15%	Activity measurements, cross section fission yields, saturation factor, deviation from average fluence value
In the reactor vessel at maximum location for cycles 1 through 6 of Davis Besse Unit 1	± 21%	Activity measurements, cross sections, fission yields, factors, axial factor, capsule location, radial/azimuthal extrapolation, normalization factor
In the reactor vessel at the maximum location for end-of-life extrapolation	± 23%	Factors in vessel fluence above plus uncertainties for extrapolation to 32 EFPY

Figure 6-2. Fast Flux, Fluence, and DPA Distribution Through Reactor Vessel Wall

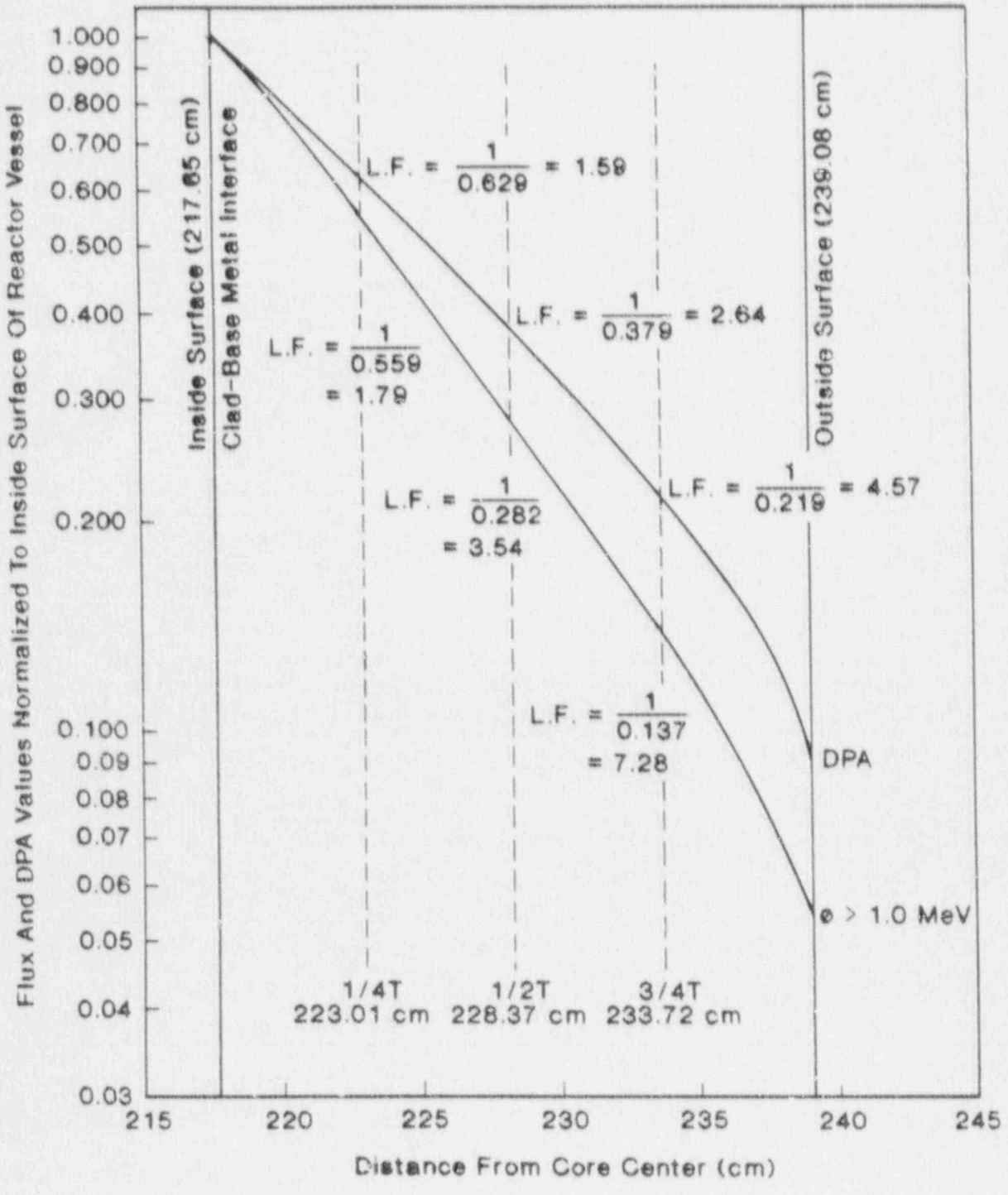

Figure 6-3. Azimuthal Flux and Fluence Distributions at Reactor Vessel Inside Surface

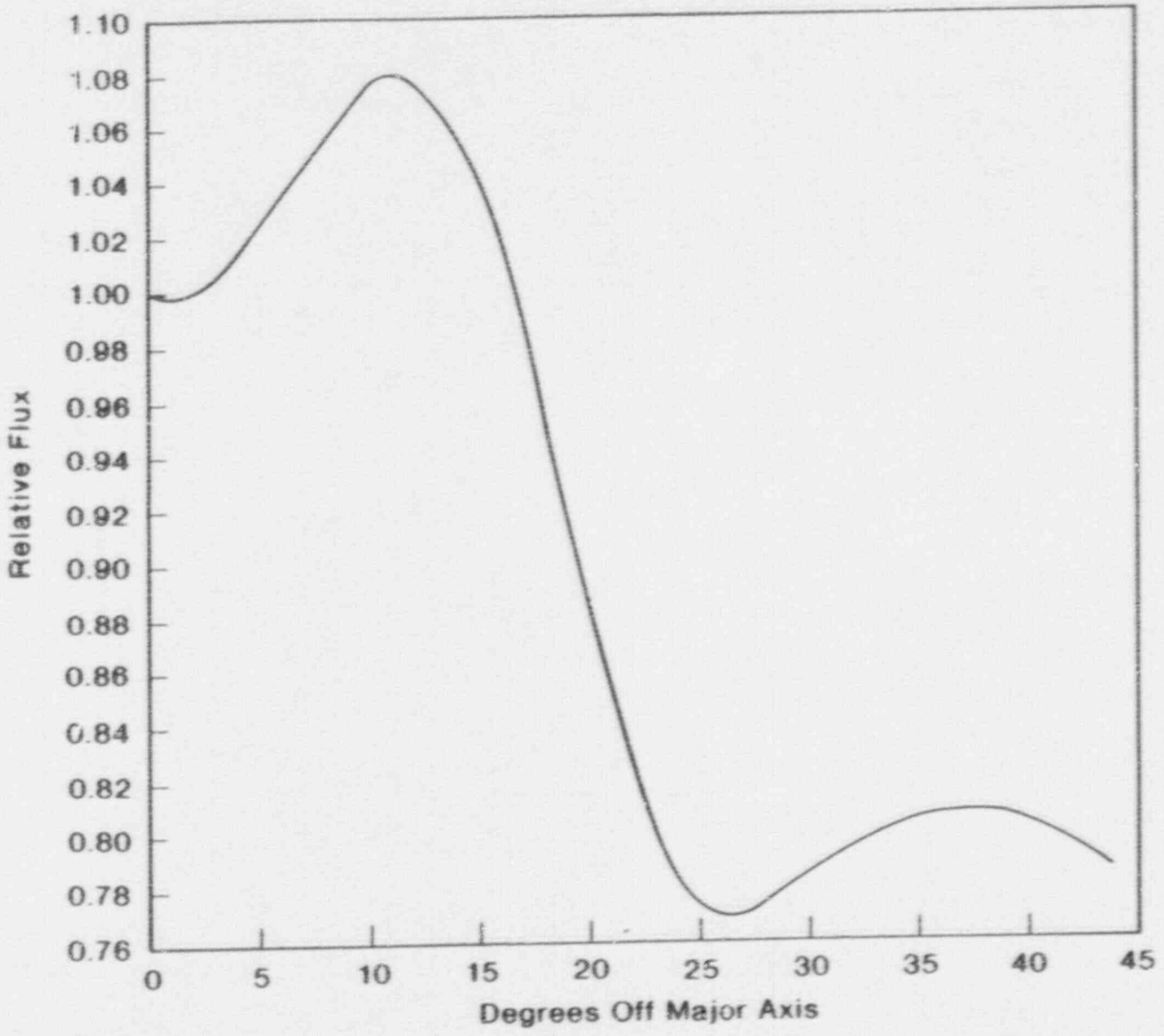

7. DISCUSSION OF CAPSULE RESULTS

7.1. Pre-Irradiation Property Data

A review of the unirradiated properties of the reactor vessel core beltline region materials indicated no significant deviation from expected properties except in the case of the upper shelf properties of the weld metal. Based on the predicted end-of-service peak neutron fluence value at the 1/4T vessel wall location and the copper content of the weld metal, it was predicted, using Regulatory Guide 1.99, Rev. 2 methodology, that the end-of-service Charpy upper shelf energy (USE) will be below 50 ft-lb. However, plant specific material surveillance data show this value will remain above 50 ft-lbs.

This weld was selected for inclusion in the surveillance program in accordance with the criteria in effect at the time the program was designed for Davis Besse Unit-1. The applicable selection criterion was based on the unirradiated properties only.

7.2. Irradiated Property Data

7.2.1. Tensile Properties

Table 7-1 compares irradiated and unirradiated tensile properties. At both room temperature and elevated temperature, the ultimate and yield strength changes in the base metal as a result of irradiation and the corresponding changes in ductility are within the limits observed for similar materials. There is some strengthening, as indicated by increases in ultimate and yield strengths and decreases in ductility properties. All changes observed in the base metal are such as to be considered within acceptable limits. The changes at both room temperature and 550F in the properties of the weld metal are larger than those observed for the base metal, indicating a greater sensitivity of the weld metal to irradiation damage. In either case, the changes in tensile properties are insignificant relative to the analysis of the reactor vessel materials at this period in service life.

A comparison of the tensile data from the first three capsules (Capsules TE1-F, TE1-A, and TE1-B) with the corresponding data from the capsule reported in this report is shown in Table 7-2. The currently reported capsule experienced a fluence that is 3/4 that of the previous capsule and five times greater than the first capsule.

The general behavior of the tensile properties as a function of neutron irradiation is an increase in both ultimate and yield strength and a decrease in ductility as measured by both total elongation and reduction of area. The most significant observation from these data is that the weld metal exhibited greater sensitivity to neutron radiation than the base metal.

7.2.2. Impact Properties

The behavior of the Charpy V-notch impact data is more significant to the calculation of the reactor system's operating limitations. Table 7-3 compares the observed changes in irradiated Charpy impact properties with the predicted changes.

The 30 ft-lb transition temperature shift for the base metal is not in good agreement with the value predicted using either Regulatory Guide 1.99, Rev. 2^{20} or Rev. 2 plus margin. It would be expected that these values would exhibit better agreement when it is considered that the data used to develop Regulatory Guide 1.99, Rev. 2, was taken at the 30 ft-lb temperature.

The transition temperature measurements at 30 ft-lbs for the weld metal is in good agreement with the results using Regulatory Guide 1.99, Revision 2, but is in poor agreement with the results using Regulatory Guide 1.99, Revision 2 plus margin. At the 30 ft-lb level, the shift relationship to the predicted value demonstrates that the estimating curves of Regulatory Guide 1.99, Rev. 2 are conservative for predicting the 30 ft-lb transition temperature shifts.

The 50 ft-lb transition temperature shift for the base metal is not in good agreement with the shift that would be predicted according to Regulatory Guide 1.99, Rev. 2. The less than ideal comparison may be attributed to the spread in the data of the material was based only on the 30 ft-lb transition data combined

with a small number of data points to establish the irradiated curve. Under these conditions, the comparison indicates that the estimating curves in RG 1.99 for low-copper materials are not conservative for predicting the 50 ft-lb transition temperature shifts.

The data for the decrease in Charpy USE with irradiation showed good agreement with predicted values for the base metal and only fair agreement for the weld metal. However, a good comparison of the measured data with the predicted value is not expected in view of the lack of data for low-, medium-, or high-copper-content materials at these fluence values that were used to develop the estimating curves.

A comparison of the Charpy impact data from the first, second and third capsules (Capsules TE1-F, TE1-A and TE1-B) with the corresponding data from the capsule reported in this report is shown in Table 7-4. The currently reported data experienced a fluence that is 3/4 that of the previous capsule and five times greater than the first capsule.

The base metal exhibited shifts at the 30 ft-lb level for the latest capsule that were greater than those of the second capsules and less than that recorded for the third capsule. The corresponding data for the weld metal showed about a 20% increase at the 30 ft-lb level.

Both the base metal and the weld metal exhibited decreases in the upper shelf values comparable to that observed in the previous capsules. These data confirm that the upper-shelf drop for this weld metal may have reached a stabilized condition (saturation) as observed in the results of capsules evaluated by others. This lack of further decrease in Charpy USE drop for this weld metal should not be considered indicative of a similar lack of decrease of upper shelf region fracture toughness properties. This behavior indicates that other reactions may be taking place within the material besides simple neutron damage. Verification of this relationship must await the testing and evaluation of the data from compact fracture toughness test specimens.

Results from other surveillance capsules also indicate that RT_{NDT} estimating curves have greater inaccuracies than originally thought. These inaccuracies are a function of a number of parameters related to the basic data available at the time the estimating curves are established. These parameters may include inaccurate fluence values, poor chemical composition values, and variations in data interpretation. The change in the regulations requiring the shift measurement to be based on the 30 ft-lb value has minimized the errors that result from using the 30 ft-lb data base to predict the shift behavior at 50 ft-lbs.

The design curves for predicting the shift will continue to be modified as more data become available; until that time, the design curves for predicting the RT_{NDT} shift as given in Regulatory Guide 1.99, Revision 2, are considered adequate for predicting the RT_{NDT} shift of those materials for which data are not available. These curves will be used to establish the pressure-temperature operational limitations for the irradiated portions of the reactor vessel until the time that new prediction curves are developed and approved.

The lack of good agreement of the change in Charpy USE is further support of the inaccuracy of the prediction curves as included in Regulatory Guide 1.99, Revision 2. Although the prediction curves are conservative in that they generally predict a larger decrease in upper-shelf energy than is observed for a given fluence and copper content, the conservatism can unduly restrict the operational limitations. These data support the contention that the USE drop curves will have to be revised as more reliable data become available; until that time the design curves used to predict the decrease in USE of the controlling materials for licensing applications are considered conservative.

7.3. Reactor Vessel Fracture Toughness

An evaluation of the reactor vessel end-of-life fracture toughness and the pressurized thermal shock criterion was made and the results are presented in Table 7-5.

The fracture toughness evaluation shows that the controlling weld metal may have an end-of-life RT_{NDT} of 216F based on Regulatory Guide 1.99, Revision 2. This predicted shift is excessive since the latest capsule (Capsule TE1-D) exhibited a measured shift of 150F for a fluence of 9.62×10^{18} n/cm^2. Ratioing this measured shift to the T/4 wall location fluence, it is estimated that the end-of-life RT_{NDT} shift will be significantly less than the value predicted using Regulatory Guide 1.99, Revision 2. This reduced shift permits the calculation of less restrictive pressure temperature operating limitations than if Regulatory Guide 1.99, Revision 2, was used.

The pressurized thermal shock evaluation demonstrates that the Davis Besse reactor pressure vessel is well below the screening criterion limits and, therefore, need not take any additional corrective action as required by the regulation.

An evaluation of the reactor vessel end-of-life upper shelf energy for each of the materials used in the fabrication was made and the results are presented in Table 7-6. This evaluation was made because the weld metals used to fabricate the reactor vessel are Linde 80 flux, low-upper-shelf-energy, relative high copper and are expected to be highly sensitive to neutron radiation damage. Two methods were used to evaluate the radiation induced decrease in upper shelf energy. The method of Regulatory Guide 1.99, Revision 2, which is the same procedure as used in Revision 1, and the method presented in BAW-1803[21] which was developed specifically to address the need of an estimating method for this class of weld metals.

The methods of both Regulatory Guide 1.99, Revision 2, and BAW-1803 show that none of the materials used in the fabrication of the reactor vessel will have an upper-shelf energy below 50 ft-lbs through 32 EFPY design life based on the T/4 wall location. Regulatory Guide 1.99 method predicts a decrease below 50 ft-lbs for the controlling weld metal at the vessel inside wall. Contrary to this prediction, the actual weld metal surveillance data does not support such a large decrease in upper-shelf energy.

Based on the Davis Besse surveillance data and the prediction techniques presented in BAW-1803, it is concluded that none of the reactor vessel material upper-shelf energies will decrease to below 50 ft-lbs during the vessel design life.

Table 7-1. Comparison of Tensile Test Results

	Room Temp. Test		Elevated Temp. Test (550F)	
	Unirr	Irrad	Unirr	Irrad
Base Metal -- ANK-191, Transverse				
Fluence, 10^{18} n/cm^2 (E > 1 MeV)	0	9.62	0	9.62
Ultimate tensile strength, ksi	90.7	95.2	86.3	91.9
0.2% yield strength, ksi	72.3	73.8	64.0	69.5
Total elongation, %	28	25	26	22
RA, %	68	61	65	58
Weld Metal -- WF-182-1				
Fluence, 10^{18} n/cm^2 (> 1 MeV)	0	9.62	0	9.62
Ultimate tensile strength, ksi	85.6	103.3	83.2	94.8
0.2% yield strength, ksi	70.2	87.3	67.6	78.1
Total elongation, %	27	25	19	18
RA, %	64	56	50	48

Table 7-2. Summary of Davis Besse Unit 1 Reactor Vessel Surveillance Capsules Tensile Test Results

Material	Fluence 10^{18} n/cm^2	Test Temp, F	Strength, ksi				Ductility, %			
			Ultimate	%(*)	Yield	%(*)	Total Elon.	%(*)	Reduction of Area	%(*)
Base Metal (BCC-241)	0	73	90.7	-	72.3	-	28	-	68	-
		580	86.3	-	64.0	-	26	-	65	-
	1.96	70	95.6	+ 5.4	75.0	+ 3.7	26	- 7.1	66	- 2.3
		580	88.8	+ 2.9	66.3	+ 3.6	22	-15.4	59	- 9.2
	5.92	76	91.1	+ 0.4	70.1	- 3.0	26	- 7.1	65	- 4.4
		580	87.5	+ 1.4	66.9	+ 4.5	21	-19.2	57	-14.0
	9.62	70	95.2	+ 5.0	73.8	+ 2.1	25	-10.7	61	-10.3
		550	91.9	+ 6.5	69.5	+ 8.6	22	-15.4	58	-10.8
	12.90	69	96.4	+ 6.3	74.7	+ 3.3	25	-10.7	65	- 4.4
		580	92.4	+ 7.0	72.2	+12.8	23	-11.5	65	0.0
Weld Metal (WF-182-1)	0	73	85.6	-	70.2	-	27	-	64	-
		580	83.2	-	67.6	-	19	-	50	-
	1.96	70	98.1	+14.6	82.5	+17.5	25	- 7.4	58	- 9.4
		580	90.0	+ 8.2	73.1	+ 8.1	21	+15.8	48	- 4.2
	5.92	76	110.9	+17.8	85.5	+21.8	16	-40.7	54	-15.6
		580	93.9	+12.8	77.8	+15.1	15	-21.0	42	-16.0
	9.62	70	103.3	+20.7	87.3	+24.4	25	- 7.4	56	-12.5
		550	94.8	+13.9	78.1	+15.5	18	- 5.3	48	- 4.0
	12.90	69	104.1	+21.6	88.8	+26.5	23	-14.8	53	-14.1
		550	96.4	+15.9	79.4	+17.5	17	-37.0	49	- 2.0

(*) Change relative to unirradiated.

Table 7-3. Observed Vs. Predicted Changes in Irradiated Charpy Impact Properties - 9.62×10^{18} n/cm^2

Material	Observed	Predicted RG 1.99/2[a]	Predicted RG 1.99/2+M[b]
Increase in 30 ft-lb Trans. Temp., F			
Base material (BCC-241)			
Transverse	3	20	40
Heat-affected zone (BCC-241)	101	20	40
Weld metal (WF-182-1)	150	167	223
Increase in 50 ft-lb Trans. Temp., F			
Base Material (BCC-241)			
Transverse	30	20	40
Heat-affected zone (BCC-241)	67	20	40
Weld metal (WF-182-1)	149	167	223
Decrease in Charpy USE, ft-lb			
Base material (BCC-241)			
Transverse	5	12	N.A.
Heat-affected zone (BCC-241)	7	12	N.A.
Weld metal (WF-182-1)	16	25	N.A.

[a] Per R.G. 1.99, Revision 2, May 1988.

[b] Per R.G. 1.99, Revision 2, May 1988, shift plus 2 x margin.

Table 7-4. Summary of Davis Besse Unit 1 Reactor Vessel Surveillance Capsules Charpy Impact Test Results

Material	Fluence 10^{18} n/cm^2	Transition Temperature Increase, F				Upper Shelf Energy, ft-lb		
		30 ft-lb Observed	Predicted[a] RG 1.99/2 w/o M	Predicted[b] RG 1.99/2 w/M	Predicted[c] BAW-1803/1	Observed	Predicted RG 1.99/2[a]	Predicted BAW-1803/1[c]
Base Metal (BCC-241)	1.96	Neg.	12	24	N.A.	113	113	N.A.
	5.92	Neg.	17	34	N.A.	113	111	N.A.
	9.62	3	20	40	N.A.	117	110	N.A.
	12.90	28	22	44	N.A.	118	108	N.A.
HAZ Metal (BCC-241)	1.96	43	12	24	N.A.	118	115	N.A.
	5.92	57	17	34	N.A.	105	113	N.A.
	9.62	101	20	40	N.A.	117	112	N.A.
	12.90	34	22	44	N.A.	111	110	N.A.
Weld Metal (WF-182-1)	1.96	127	96	152	80	62[d]	53	64
	5.92	125	144	200	140	55[d]	48	61
	9.62	150	167	223	166	54	46	60
	12.90	175	181	237	182	54[d]	44	59

[a] Per Regulatory Guide 1.99, Revision 2, dated May 1988.

[b] Per Regulatory Guide 1.99, Revision 2, plus margin.

[c] Per BAW-1803, Revision 1, dated October 1990, plus margin.

[d] Upper-shelf energy value re-defined per ASTM E185.

Table 7-5. Evaluation of Reactor Vessel End-of-Life Fracture Toughness and Pressurized Thermal Shock Criterion

Material Description			Material Chemical Composition		Estimated EOL Fluence		T/4 Wall EOL RT_{NDT}, F		PTS Evaluation, F	
Reactor Vessel Beltline Region Location	Heat Number	Type	Copper, w/o	Nickel, w/o	Inside Surface n/cm^2	T/4 Wall Location n/cm^2	Per RG 1.99/2[a]	Per BAW-1083/1	EOL RT_{PTS}[c]	Screening Criterion[c]
Nozzle Belt	ADR-203	SA508, C1.2	0.04	0.68	2.64E18	1.59E18	86	N.A.	101	270
Upper Shell	AKJ-233	SA508, C1.2	0.04	0.77	1.11E19	6.67E18	65	N.A.	81	270
Lower Shell	BCC-241	SA508, C1.2	0.02	0.81	1.11E19	6.67E18	56	N.A.	105	270
Upper Circum. Seam (ID9%)	WF-232	Weld	0.18	0.64	2.64E18	--	N.A.	N.A.	169	300
Upper Circum. Seam (OD91%)	WF-233	Weld	0.29	0.63	--	1.59E18	168	208	N.A.	300
Mid. Circum. Seam (100%)	WF-182-1	Weld	0.24	0.63	1.11E19	6.67E18	216	167	211	300
Lower Circum. Seam (ID12%)	WF-232	Weld	0.18	0.64	1.34E16	--	N.A.	N.A.	70	300
Lower Circum. Seam (OD88%)	WF-233	Weld	0.29	0.68	--	8.05E15	Neg.	Neg.	N.A.	300

(a) Per Regulatory Guide 1.99, Revision 2, dated May 1988.

(b) Per Regulatory Guide 1.99, Revision 1, dated April 1977.

(c) Per 10CFR50, Section 50.61, Fracture Toughness Requirements for Protection Against Pressurized Thermal Shock Events with proposed changes to make it consistant with Regulatory Guide 1.99, Revision 2, May 1988 (proposed revision published in Federal Register, Vol. 54, No. 246, December 26, 1989).

Table 7-6. Evaluation of Reactor Vessel End-of-Life Upper Shelf Energy

Material Description			Material Chemical Composition		Estimated EOL Fluence		Initial USE, ft-lbs	Estimated EOL USE Per RG 1.99/2[a]		Estimated EOL USE Per BAW-1803[b]		Estimated EFPY to 50 ft-lbs at T/4 Wall RG 1.99/2
Reactor Vessel Beltline Region Location	Heat Number	Type	Copper, w/o	Nickel, w/o	Inside Surface n/cm^2	T/4 Wall Location n/cm^2		Inside Surface	T/4 Wall Location	Inside Surface	T/4 Wall Location	
Nozzle Belt	ADB-203	SA508, Cl.2	0.04	0.68	2.64E18	1.59E18	133[c]	121	122	N.A.	N.A.	>32
Upper Shell	AKJ-233	SA508, Cl.2	0.04	0.77	1.11E19	6.67E18	140[c]	120	124	N.A.	N.A.	>32
Lower Shell	BCC-241	SA508, Cl.2	0.02	0.81	1.11E19	6.67E18	118[c]	105	107	N.A.	N.A.	>32
Upper Circum. Seam (ID9%)	WF-232	Weld	0.18	0.64	2.64E18	--	(70)[b]	53	-	67	--	>32
Upper Circum. Seam (OD91%)	WF-233	Weld	0.29	0.68	--	1.59e18	(70)[b]	-	50	--	58	>32
Mid. Circum. Seam (100%)	WF-182-1	Weld	0.24	0.63	1.11E19	6.67E18	81[c]	49	53	58	59	>32
Lower Circum. Seam (ID12%)	WF-232	Weld	0.18	0.64	1.34E16	--	(70)[b]	N.A.	-	N.A.	--	>32
Lower Circum. Seam (OD88%)	WF-233	Weld	0.29	0.68	--	8.05E15	(70)[b]	-	N.A.	--	N.A.	>32

[a] Per Regulatory Guide 1.99, Revision 2, dated May 1988.

[b] Per BAW-1803, Revision 1, dated October 1990.

[c] Per Certified Materials Test Reports.

8. DETERMINATION OF REACTOR COOLANT PRESSURE BOUNDARY PRESSURE - TEMPERATURE LIMITS

The pressure-temperature limits of the reactor coolant pressure boundary (RCPB) of Davis Besse Unit-1 are established in accordance with the requirements of 10CFR50, Appendix G. The methods and criteria employed to establish operating pressure and temperature limits are described in topical report BAW-10046A.[24] The objective of these limits is to prevent nonductile failure during any normal operating condition, including anticipated operation occurrences and system hydrostatic tests. The loading conditions of interest include the following:

1. Normal operations, including heatup and cooldown.
2. Inservice leak and hydrostatic tests.
3. Reactor core operation.

The major components of the RCPB have been analyzed in accordance with 10CFR50, Appendix G. The closure head region, the reactor vessel outlet nozzle, and the beltline region have been identified as the only regions of the reactor vessel (and consequently of the RCPB) that regulate the pressuretemperature limits. Since the closure head region is significantly stressed at relatively low temperatures (due to mechanical loads resulting from bolt preload), this region largely controls the pressure-temperature limits of the first several service periods. The reactor vessel outlet nozzle also affects the pressure-temperature limit curves of the first several service periods. This is due to the high local stresses at the inside corner of the nozzle, which can be two to three times the membrane stresses of the shell. After the first several years of neutron radiation exposure, the RT_{NDT} of the beltline region materials will be high enough that the beltline region of the reactor vessel will start to control the pressure-temperature limits of the RCPB. For the service period for which the

limit curves are established, the maximum allowable pressure as a function of fluid temperature is obtained through a point-by-point comparison of the limits imposed by the closure head region, the outlet nozzle, and the beltline region. The maximum allowable pressure is taken to be the lowest of the three calculated pressures.

The limit curves for Davis Besse Unit 1 are based on the predicted values of the adjusted reference temperatures of all the beltline region materials at the end of the thirty-second EFPY. The thirty-second EFPY was selected because it is estimated that the fourth surveillance capsule will be withdrawn at the end of the refueling cycle when the estimated capsule fluence corresponded to approximately the inside surface end-of-life value. The time difference between the withdrawal of the third and fourth surveillance capsule provides adequate time for re-establishing the operating pressure and temperature limits for the period of operation beyond the current limits.

The unirradiated impact properties were determined for the surveillance beltline region materials in accordance with 10CFR50, Appendixes G and H. For the other beltline region and RCPB materials for which the measured properties are not available, the unirradiated impact properties and residual elements, as originally established for the beltline region materials, are listed in Table A-1. The adjusted reference temperatures are calculated by adding the predicted radiation-induced RT_{NDT} and the unirradiated RT_{NDT}. The predicted RT_{NDT} is calculated using the respective neutron fluence and copper and nickel contents. Figure 8-1 illustrates the calculated peak neutron fluence at several locations through the reactor vessel beltline region wall. The supporting information for Figure 8-1 is described in Section 6. The neutron fluence values of Figure 8-1 are the predicted fluences that have been demonstrated (Section 6) to be conservative. The design curves of Regulatory Guide 1.99, Rev. 2, were used to predict the radiation-induced RT_{NDT} values as a function of the material's copper and nickel content and neutron fluence.

The neutron fluences and adjusted RT_{NDT} values of the beltline region materials at the end of the thirty-second full-power year are listed in Table 8-1. The

neutron fluences and adjusted RT_{NDT} values are given for the 1/4T and 3/4T vessel wall locations (T = wall thickness). The assumed RT_{NDT} of the closure head region and the outlet nozzle steel forgings is 60F, in accordance with BAW-10046.

The chemistry factors for the controlling metals (WF-182-1) in the beltline region was recalculated in accordance with the procedures described in Regulatory Guide 1.99, Revision 2, Regulatory Position 2.

The data used to calculate a new chemistry factor for weld metal WF-182-1 was obtained from the B&WOG Integrated Reactor Vessel Surveillance Program. The data for the weld metal WF-182-1 which has the weld wire Heat No. 821T44. A summary of the available data is as follows.

Capsule	Weld Metal	Fluence, n/cm^2	ΔRT_{NDT}, F	Reference
TE1-F	WF-182-1	1.96E+18	127	1
TE1-B	WF-182-1	5.92E+18	125	2
TE1-D	WF-182-1	9.62E+19	150	(This report)
TE1-A	WF-182-1	1.29E+19	175	3

The analysis of these data produced a new chemistry factor for WF-182-1 of 162.

Similarly, the data used to calculate a new chemistry factor for weld metal WF-233 was obtained from the B&WOG IRVSP (Integrated Reactor Vessel Surveillance Program). The data for weld metal WF-233 has the weld wire Heat No. T29744. A summary of the available data is as follows.

Capsule	Weld Metal	Fluence, n/cm^2	ΔRT_{NDT}, F	Reference
Ko-Ri 1-V	WF-233	4.67E+18	191	22
Ko-Ri 1-T	WF-233	1.08E+19	187	22
Ko-Ri 1-S	WF-233	1.21E+19	222	22

The analysis of these data produced a new chemistry factor for WF-233 of 207.

Figure 8-2 shows the reactor vessel's pressure-temperature limit curve for normal heatup. This figure also shows the the core criticality limits as required by 10CFR50, Appendix G. Figures 8-3 and 8-4 show the vessel's pressure-temperature limit curve for normal cooldown and for heatup during inservice leak and hydrostatic tests, respectively. All pressure-temperature limit curves are applicable up to the thirty-second EFPY. Protection against nonductile failure is ensured by maintaining the coolant pressure below the upper limits of the pressure-temperature limit curves. The acceptable pressure and temperature combinations for reactor vessel operation are below and to the right of the limit curve. The reactor is not permitted to go critical until the pressure-temperature combinations are to the right of the criticality limit curve. To establish the pressure-temperature limits for protection against nonductile failure of the RCPB, the limits presented in Figures 8-2 through 8-4 must be adjusted by the pressure differential between the point of system pressure measurement and the pressure on the reactor vessel controlling the limit curves. This is necessary because the reactor vessel is the most limiting component of the RCPB.

Table 8-1. Data for Preparation of Pressure-Temperature Limit Curves for Davis Besse Unit 1 -- Applicable Through 32 EFPY

Material Identification		Beltline Region Location	Weldment Location			Inside Surface Fluence	Chemical Composition[c]		Chemistry Factor	Initial RT_{NDT}, F	Radiation Induced ΔRT_{NDT} at End of 32 EFPY, F		Margin, F	Adjusted RT_{NDT} at End of 32 EFPY[a], F	
Heat No	Type		Core Midplane to Weld cm	Location from Major Axis Degrees	Weld T/4 Location	n/cm^2	Copper, w/o	Nickel, w/o			1/4	3T/4		1/4	3T/4
ADB 203	SA508, Cl 2	Nozzle belt	--	--	--	2.64E18	0.04	0.68	26	+50[g]	13	8	7/4	70	60
AKJ 233	SA508, Cl 2	Upper shell	--	--	--	1.11E19	0.04	0.77	26	+20[g]	23	16	12/8	55	44
BCC 241	SA508, Cl 2	Lower shell	--	--	--	1.11E19	0.02	0.81	20	+50[g]	18	12	9/6	77	68
WF 232	ASA/Linde 80	Upper circum weld (ID 9%)	+198	--	No	2.64E18	0.18	0.64	161	6[b]	83	51	69/65	146	110
WF 233	ASA/Linde 80	Upper circum weld (OD 91%)	+198	--	Yes	2.64E18	0.29	0.68	204	6[b]	105	64	69/69	168	127
WF 182-1	ASA/Linde 80	Middle circum weld (100%)	24	--	Yes	1.11E19	0.24	0.63	178	+2[g]	158	109	56/56	(216)[d]	(167)[d]
WF 232	ASA/Linde 80	Lower circum weld (ID 12%)	-247	--	No	1.34E16	0.18	0.64	161	6[b]	--	--	--	--	--
WF 233	ASA/Linde 80	Lower circum weld (OD 88%)	-247	--	Yes	1.34E16	0.29	0.68	--	6[b]	--	--	--	--	--
WF 182-1	ASA/Linde 80	Calculated RT_{NDT} shift of limiting weld metal based on use of surveillance capsule data per Regulatory Guide 1.99, Revision 2, Regulatory Position 2.1.				1.11E19	--	--	162	+2[g]	144	99	28/28	(174)[e]	(129)[e]
WF 233	ASA/Linde 80	Calculated RT_{NDT} shift of limiting weld metal based on use of surveillance capsule data per Regulatory Guide 1.99, Revision 2, Regulatory Position 2.1.				2.64E18	--	--	207	6[b]	107	65	34/34	135	93

[a] RT_{NDT} calculated per Regulatory Guide 1.99, Revision 2, dated May 1988.

[b] Estimated initial RT_{NDT} of weld metals per BAW-1803, Revision 1, October 1990; One Standard Deviation = 20F

[c] Materials chemical compositions per BAW-1820, December 1984[23] and BAW-1799, July 1983.[24]

[d] Initial calculated RT_{NDT} values for use in calculation of pressure temperature limits.

[e] RT_{NDT} values used to calculate pressure temperature limits.

[f] Reactor vessel wall thickness = 8.5 inches.

[g] Per Certified Material Test Reports.

Figure 8-1. Predicted Fast Neutron Fluence at Various Locations Through Reactor Vessel Wall for 32 EFPY - Davis Besse Unit 1

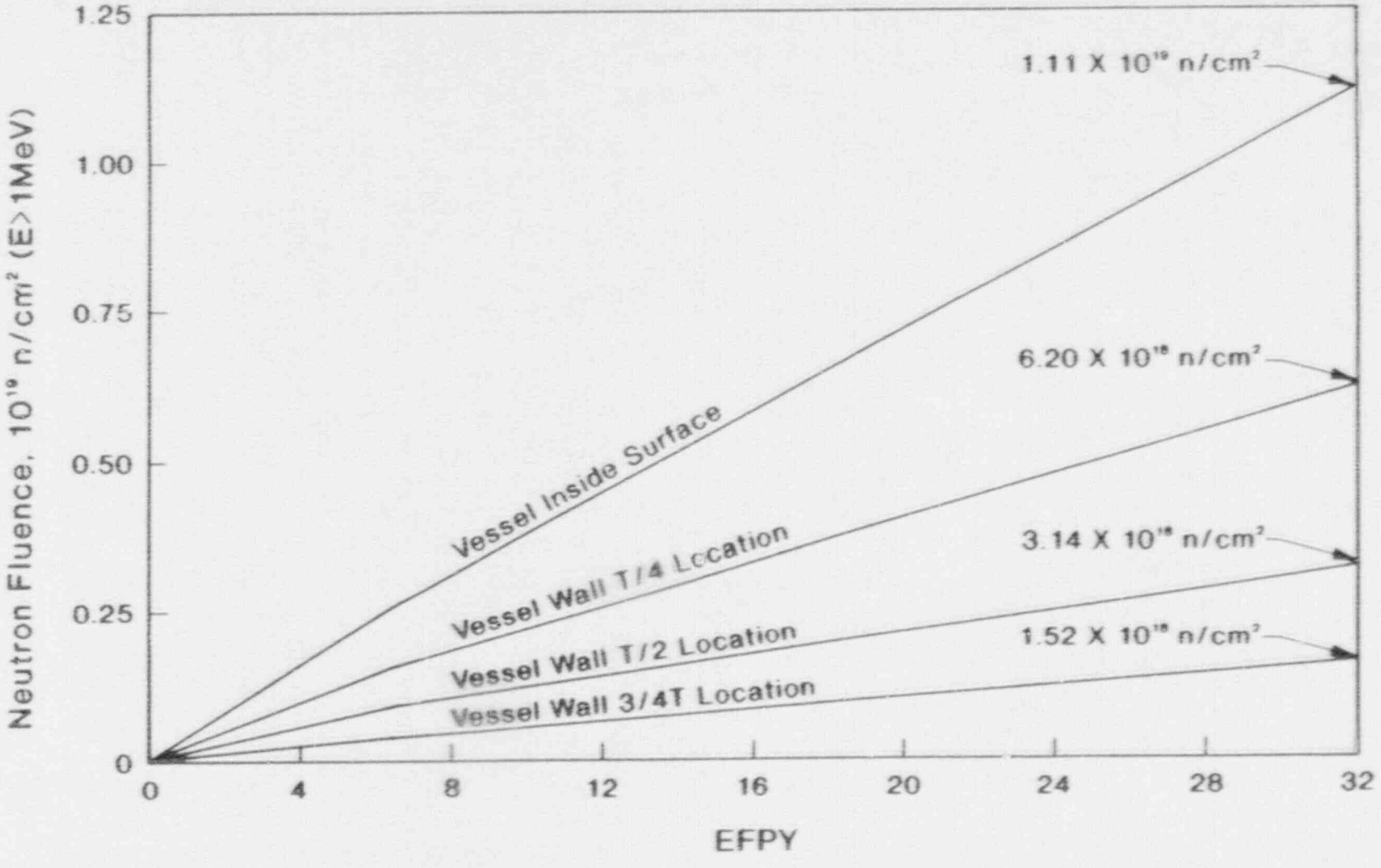

Figure 8-2. Reactor Vessel Pressure-Temperature Limit Curves for Normal Operation - Heatup, Applicable for First 32 EFPY - Davis Besse Unit 1

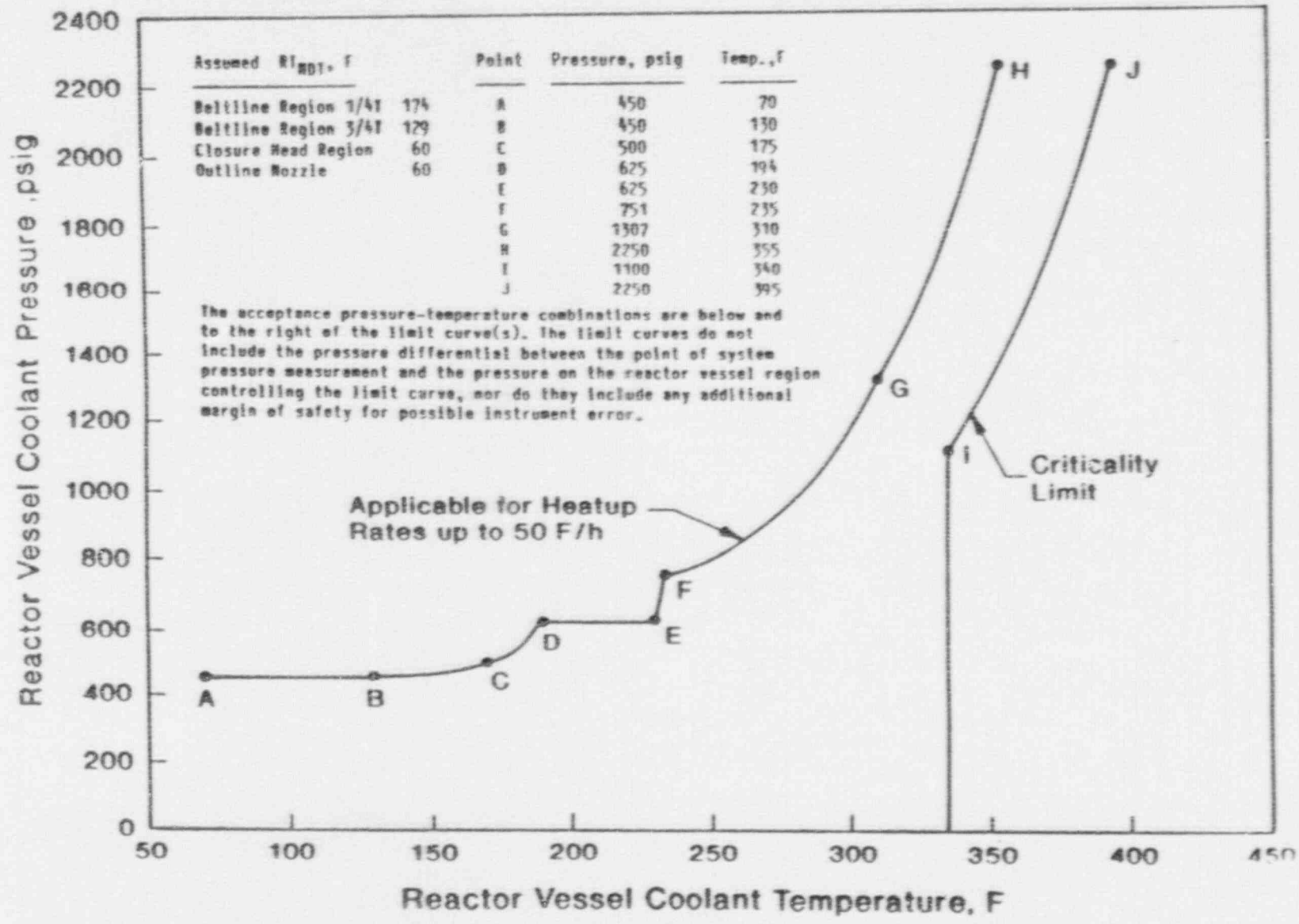

Figure 8-3. Reactor Vessel Pressure-Temperature Limit Curves for Normal Operation - Cooldown, Applicable for First 32 EFPY - Davis Besse 1

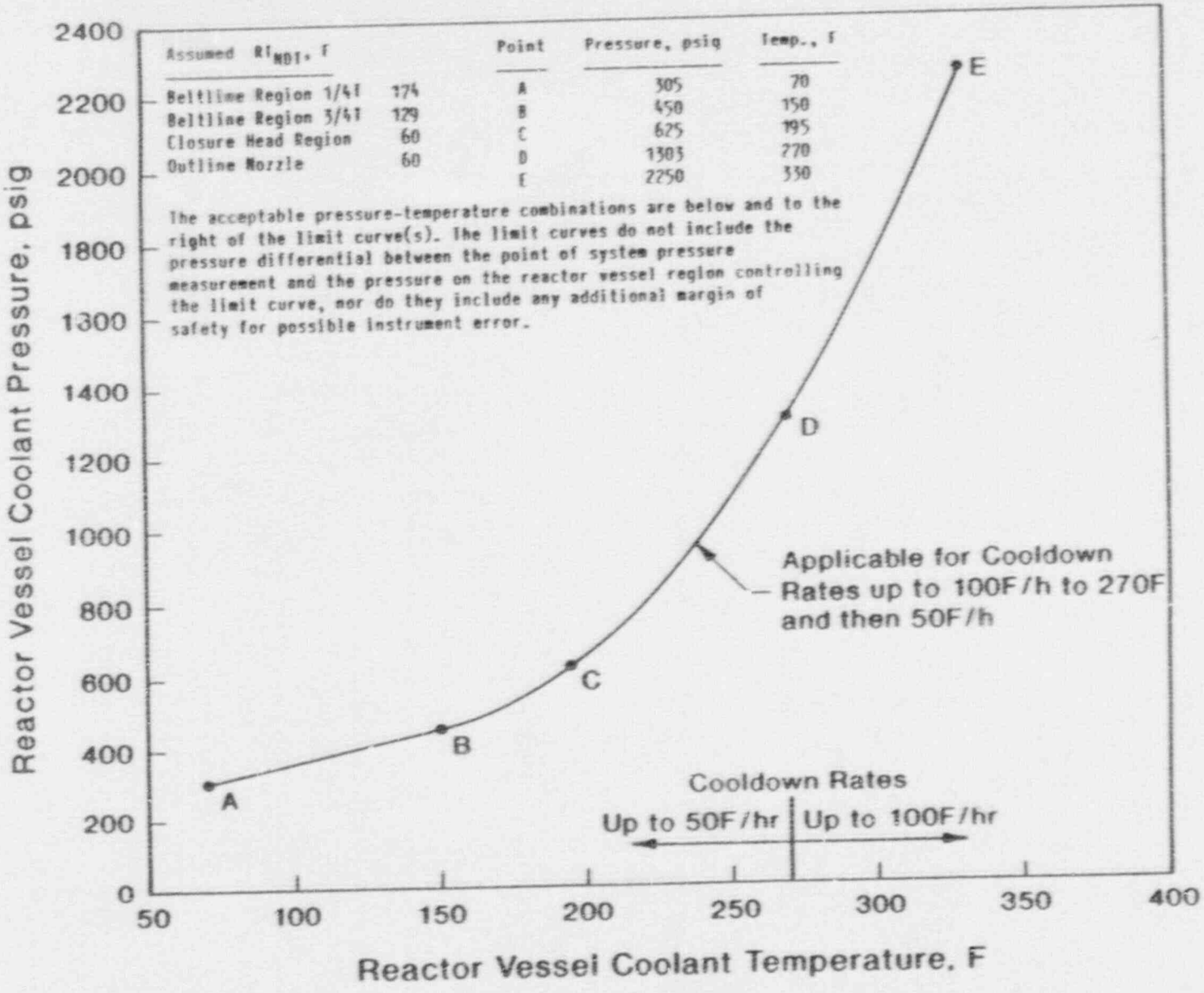

Figure 8-4. Reactor Vessel Pressure-Temperature Limit Curves for Inservice Leak and Hydrostatic Tests, Applicable for First 32 EFPY - Davis Besse Unit 1

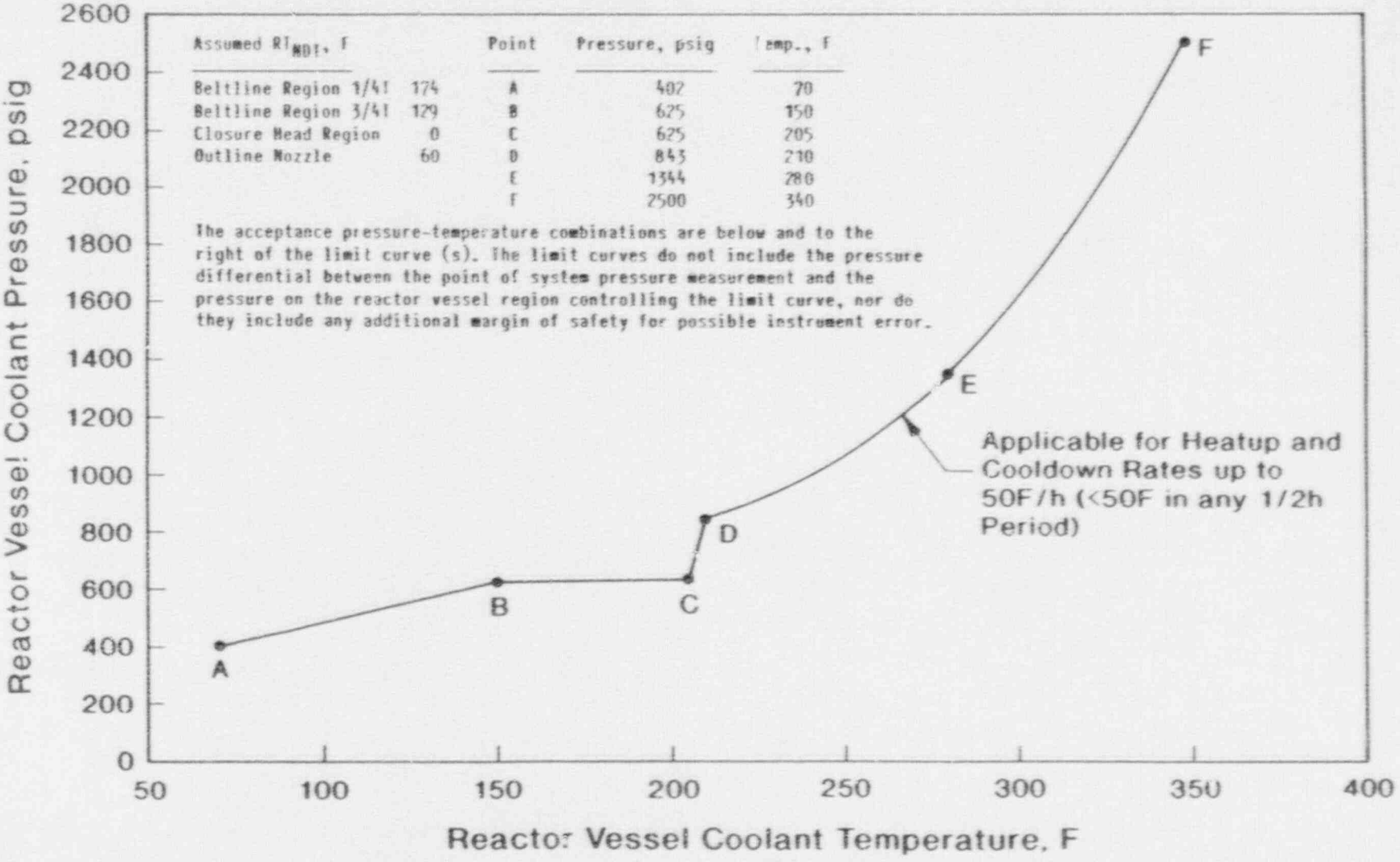

9. SUMMARY OF RESULTS

The analysis of the reactor vessel material contained in the third surveillance capsule, TEJ-D, removed for evaluation as part of the Davis Besse Unit 1 Reactor Vessel Surveillance Program, led to the following conclusions:

1. The capsule received an average fast fluence of 9.62×10^{18} n/cm^2 (E > 1.0 MeV). The predicted fast fluence for the reactor vessel T/4 location at the end of the sixth fuel cycle is 1.36×10^{18} n/cm^2 (E > 1 MeV).

2. The fast fluence of 9.62×10^{18} n/cm2 (E > 1 MeV) increased the RT_{NDT} of the capsule reactor vessel core region shell materials a maximum of 150F.

3. Based on the calculated fast flux at the vessel wall, an 80% capacity factor and the planned fuel management, the projected fast fluence that the Davis Besse Unit 1 reactor pressure vessel inside surface will receive in 32 EFPY operation is 1.11×10^{19} n/cm^2 (E > 1 MeV).

4. The increase in the RT_{NDT} for the shell forging material was not in good agreement with that predicted by the currently used design curves of RT_{NDT} versus fluence (i.e., R.G. 1.99/Rev. 2).

5. The increase in the RT_{NDT} for the weld metal was in good agreement with that predicted by the currently used design curves of RT_{NDT} versus fluence (i.e., R.G. 1.99/Rev. 2) and the prediction techniques are conservative.

6. The RT_{PTS} values decreased for 32 EFPY because of a decrease in the estimated EOL fluence values and are well below the PTS screening criteria.

7. The current techniques (i.e., Regulatory Guide 1.99, Revision 2) used to predict the change in weld metal Charpy upper-shelf properties due to irradiation are conservative.

8. The analysis of the neutron dosimeters demonstrated that the analytical techniques used to predict the neutron flux and fluence were accurate.

9. The capsule design operating temperature may have been exceeded during operating transients but not for times and temperatures that would make the capsule data unusable.

10.0 SURVEILLANCE CAPSULE REMOVAL SCHEDULE

Based on the postirradiation test results of capsule TE1-D, the following schedule is recommended for examination of the remaining capsules in the Davis Besse Unit 1 RVSP:

Evaluation Schedule[a]

Capsule ID	Estimated Capsule Fluence, 10^{19} n/cm^2	Estimated Vessel Fluence, 10^{19} n/cm^2		Estimated Date Data Available[b]
		Surface	1/4T	
TE1-C[c]	1.9	0.24	0.14	Removed/In Storage
TE1-E[c]	1.7	0.42	0.24	1996

(a) In accordance with BAW-10100A and ASTM E 185-79 as modified by BAW-1543A, Rev. 3, September 1989.

(b) Estimated date based on 0.8 plant operation factor.

(c) Capsules designated as standbys and may not be evaluated when removed.

11. CERTIFICATION

The specimens were tested, and the data obtained from Davis Besse Nuclear Power Station Unit 1 surveillance capsule TE1-D were evaluated using accepted techniques and established standard methods and procedures in accordance with the requirements of 10CFR50, Appendixes G and H.

A. L. Lowe, Jr., P.E. — 19 Dec 1990 — Date
Project Technical Manager

This report has been reviewed for technical content and accuracy.

M. J. Devan (Material Analysis) — 19 Dec 1990 — Date
M&SA Unit

L. B. Wimmer (Fluence Analysis) — 19 DEC 90 — Date
Performance Analysis Unit

K. K. Yoon, P.E. (Fracture Analysis) — 19 Dec. 90 — Date
M&SA Unit

Verification of independent review.

K. E. Moore, Manager — 19 Dec 90 — Date
M&SA Unit

This report has been approved for release.

T. L. Baldwin — 12/19/90 — Date
Program Manager

APPENDIX A

Reactor Vessel Surveillance Program
Background Data and Information

1. Material Selection Data

The data used to select the materials for the specimens in the surveillance program, in accordance with E-185-73, are shown in Table A-1. The locations of these materials within the reactor vessel are shown in Figure A-1.

2. Definition of Beltline Region

The beltline region of Davis Besse Unit 1 was defined in accordance with the data given in BAW-10100A.

3. Capsule Identification

The capsules used in the Davis Besse Unit 1 surveillance program are identified below by identification number, type, and location.

Capsule Cross Reference Data

Number	Type
TE1-A	III
TE1-B	IV
TE1-C	III
TE1-D	IV
TE1-E	III
TE1-F	IV

4. Specimens for Determining Material Baseline Properties

See Table A-2.

5. Specimens per Surveillance Capsule

See Tables A-3 and A-4.

Table A-1. Unirradiated Impact Properties and Residual Element Content Data of Beltline Region Materials Used for Selection of Surveillance Program Materials -- Davis-Besse Unit 1

Material Ident, Heat No.	Material Type	Beltline Region Location	Distance, Core Midplane to Weld Centerline, cm	Drop wt. T_{NDT}, F	Charpy Data, CVN				RT_{NDT}, F	Chemistry, %			
					Longitudinal	Transverse							
					At 10F ft-lb	50 ft-lb, F	35 MLE, F	USE, ft-lb		Cu	P	S	Ni
ADB-203	SA508, Cl 2	Nozzle belt	--	50	--	61	--	134	50	0.04	0.007	0.009	--
AKJ-233	SA508, Cl 2	Upper Shell B	--	20	136,179,130 107,96,81	30	--	144	20	0.04	0.004	0.006	--
BCC-241	SA508, Cl 2	Lower Shell A	--	50	60,62,47 47,62,59	27	--	118	50	0.02	0.011	0.011	--
WF-232	Weld	Circum seam upper (9% ID)	+198	--	25,31,35	--	--	-	--	0.14	0.011	0.007	--
WF-233	Weld	Circum seal upper (91% OD)	+198	--	43,30,26	--	--	-	--	0.22	0.015	0.016	--
WF-182-1	Weld	Circum seam Middle	- 24	-20	36,33,44	62	--	81	2	0.18	0.014	0.015	--
WF-232	Weld	Circum seam lower (12% ID)	-247	--	25,31,35	--	--	-	--	0.14	0.011	0.007	--
WF-233	Weld	Circum seam lower (88% OD)	-247	--	43,30,26	--	--	-	--	0.22	0.015	0.016	--

Table A-2. Test Specimens for Determining Material Baseline Properties

Material Description	No. of Test Specimens			
	Tension			
	70F	600F[a]	CVN Impact	Compact Fracture[b]
Heat SS				
Base Metal				
Transverse Direction	3	3	15	--
Longidutinal Direction	3	3	15	--
Heat-Affected Zone (HAZ)				
Transverse Direction	3	3	15	--
Longitudinal Direction	3	3	15	--
Total	12	12	60	--
Heat TT				
Base Metal				
Transverse Direction	3	3	15	--
Longitudinal Direction	3	3	15	--
Heat-Affected Zone (HAZ)				
Transverse Direction	3	3	15	--
Longitudinal Direction	3	3	15	--
Total	12	12	60	--
Weld Metal				
Longitudinal Direction	3	3	15	8 1/2 TCT 4 1 TCT

[a] Testtemperature to be the same as irradiation temperature.

[b] Testtemperature to be determined from shift in impact transition curves after irradiation exposure.

Table A-3. Specimens in Upper Surveillance Capsules (Designations A, C, and E)

Material Description	No. of Test Specimens Tension	CVN Impact
Weld Metal	2	12
Weld, HAZ		
Heat SS, Transverse	-	12
Heat TT, Transverse	-	6
Base Metal		
Heat SS, Transverse	2	12
Heat TT, Transverse	-	6
Correlation Material	-	6
Total Per Capsule	4	54

Table A-4. Specimens in Lower Surveillance Capsules (Designations B, D, and F)

Material Description	No. of Test Specimens Tension	CVN Impact	1/2T Compact Fracture[a]
Weld Metal	2	12	8
Weld, HAZ			
Heat SS, Transverse	-	12	-
Base Metal			
Heat SS, Transverse	2	12	-
Total Per Capsule	4	36	8

[a] Compact fracture toughness specimens precracked per ASTM E399-72.

Figure A-1. Location and Identification of Materials Used in Fabrication of Reactor Pressure Vessel

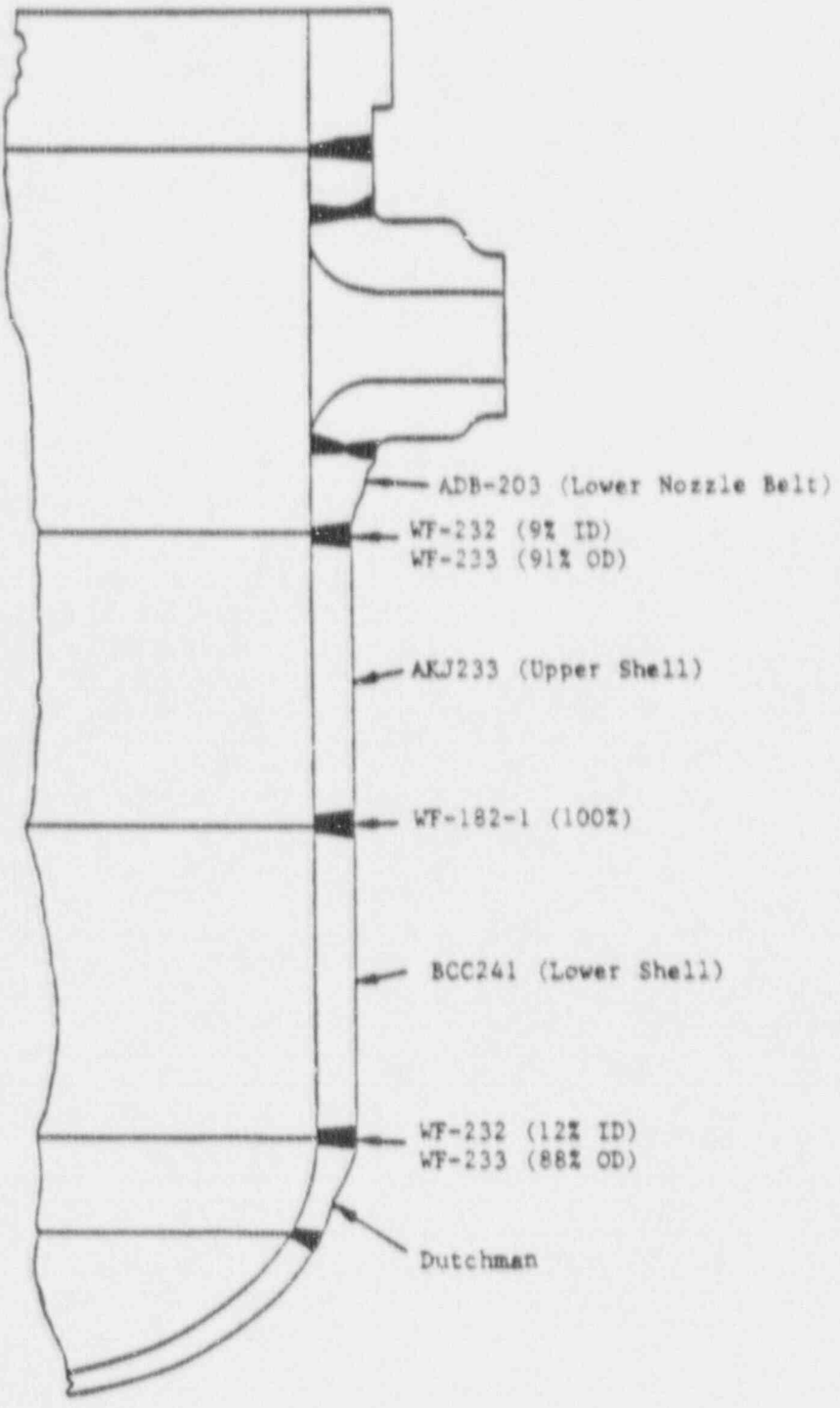

APPENDIX B

Pre-Irradiation Tensile Data

Table B-1. Pre-Irradiation Tensile Properties of Shell Plate Material, Heat BCC-241

Specimen No.	Test Temp, F	Strength, 1000 psi Yield	Strength, 1000 psi Ultimate	Elongation, % Uniform	Elongation, % Total	Red'n of Area, %
SS-601	73	75.6	91.9	12.7	27.0	67.3
603	73	69.4	90.0	13.1	27.2	67.0
604	73	71.9	90.3	13.0	28.8	71.1
Mean	73	72.3	90.7	12.9	27.7	68.5
Std. dev'n.	73	3.12	1.02	0.21	0.99	2.29
SS-606	580	64.4	86.3	14.4	25.7	65.4
611	580	64.4	86.3	13.6	26.0	63.7
615	578	63.1	86.3	16.3	25.5	67.0
Mean	580	64.0	86.3	14.8	25.7	65.4
Std. dev'n.	580	0.75	0	1.39	0.25	1.65

Table B-2. Pre-Irradiation Tensile Properties for Weld Metal WF-182-1

Specimen No.	Test Temp, F	Strength, 1000 psi Yield	Strength, 1000 psi Ultimate	Elongation, % Uniform	Elongation, % Total	Red'n of Area, %
SS-003	73	69.7	85.6	14.8	26.0	63.7
007	73	69.7	85.6	15.4	27.3	64.7
Mean	73	70.2	85.6	15.1	26.7	64.2
Std. dev'n.	73	0.64	0	0.42	0.92	0.71
SS-009	582	64.6	80.6	14.8	20.0	50.1
015	582	67.8	83.1	11.4	17.4	49.7
016	579	770.6	85.9	12.5	18.9	50.9
Mean	580	67.6	83.2	12.9	18.8	50.2
Std. dev'n.	580	3.10	2.65	1.73	1.31	0.61

APPENDIX C

Pre-Irradiation Charpy Impact Data

Table C-1. Pre-Irradiation Charpy Impact Data for Shell Forging Material - Transverse Orientation, Heat BCC-241

Specimen No.	Test Temp., F	Asborbed Energy, ft-lb	Lateral Expansion, 10^{-3} in.	Shear Fracture, %
SS-616	-79	5.5	10	0
SS-636	-40	17.5	14	0
SS-609	- 2	19.5	18	0
SS-617	0	16.5	16	0
SS-621	21	39.0	33	2
SS-666	40	53.0	45	15
SS-667	40	73.0	57	20
SS-672	40	88.0	69	60
SS-643	70	76.0	60	25
SS-646	70	87.0	70	25
SS-652	74	109.0	79	85
SS-627	106	99.0	74	80
SS-663	130	111.5	85	90
SS-686	171	120.0	88	100
SS-656	213	128.5	92	100
SS-658	278	116.0	89	100
SS-681	338	113.5	88	100
SS-630	585	113.0	83	100

Table C-2. Pre-Irradiation Charpy Impact Data for Shell Forging Material - Heat-Affected Zone, Heat BCC-241

Specimen No.	Test Temp., F	Asborbed Energy, ft-lb	Lateral Expansion, 10^{-3} in.	Shear Fracture, %
SS-331	-120	27.0	19	0
SS-307	- 80	30.5	16	0
SS-309	- 80	60.0	36	0
SS-310	- 80	28.0	17	2
SS-325	- 59	67.0	37	20
SS-346	- 40	56.0	31	10
SS-320	- 20	62.0	37	25
SS-337	20	94.0	54	30
SS-341	- 2	97.5	57	60
SS-329	40	114.5	69	40
SS-305	74	133.0	76	90
SS-333	106	135.5	88	100
SS-304	130	110.5	77	100
SS-315	176	138.5	82	100
SS-335	223	110.0	79	100
SS-343	338	112.0	83	100
SS-322	406	135.5	84	100
SS-348	578	101.0	78	100

Table C-3. Pre-Irradiation Charpy Impact Data for Weld Metal WF-182-1

Specimen No.	Test Temp., F	Asborbed Energy, ft-lb	Lateral Expansion, 10^{-3} in.	Shear Fracture, %
SS-046	-80	15.5	16	0
SS-060	-40	16.0	15	2
SS-077	- 2	37.5	35	10
SS-084	- 2	28.0	27	25
SS-053	0	33.0	29	20
SS-055	0	33.5	29	15
SS-027	40	40.0	40	50
SS-028	40	40.0	38	35
SS-029	40	37.5	34	15
SS-071	70	45.5	44	50
SS-081	70	58.0	55	70
SS-092	74	55.0	56	75
SS-056	130	70.5	64	100
SS-067	145	36.5	35	40
SS-036	169	69.5	64	100
SS-063	223	72.5	71	100
SS-085	228	66.5	65	100
SS-016	338	72.0	70	100
SS-040	583	68.5	72	100

Figure C-1. Impact Data for Unirradiated Shell Forging Material, Heat BCC-241

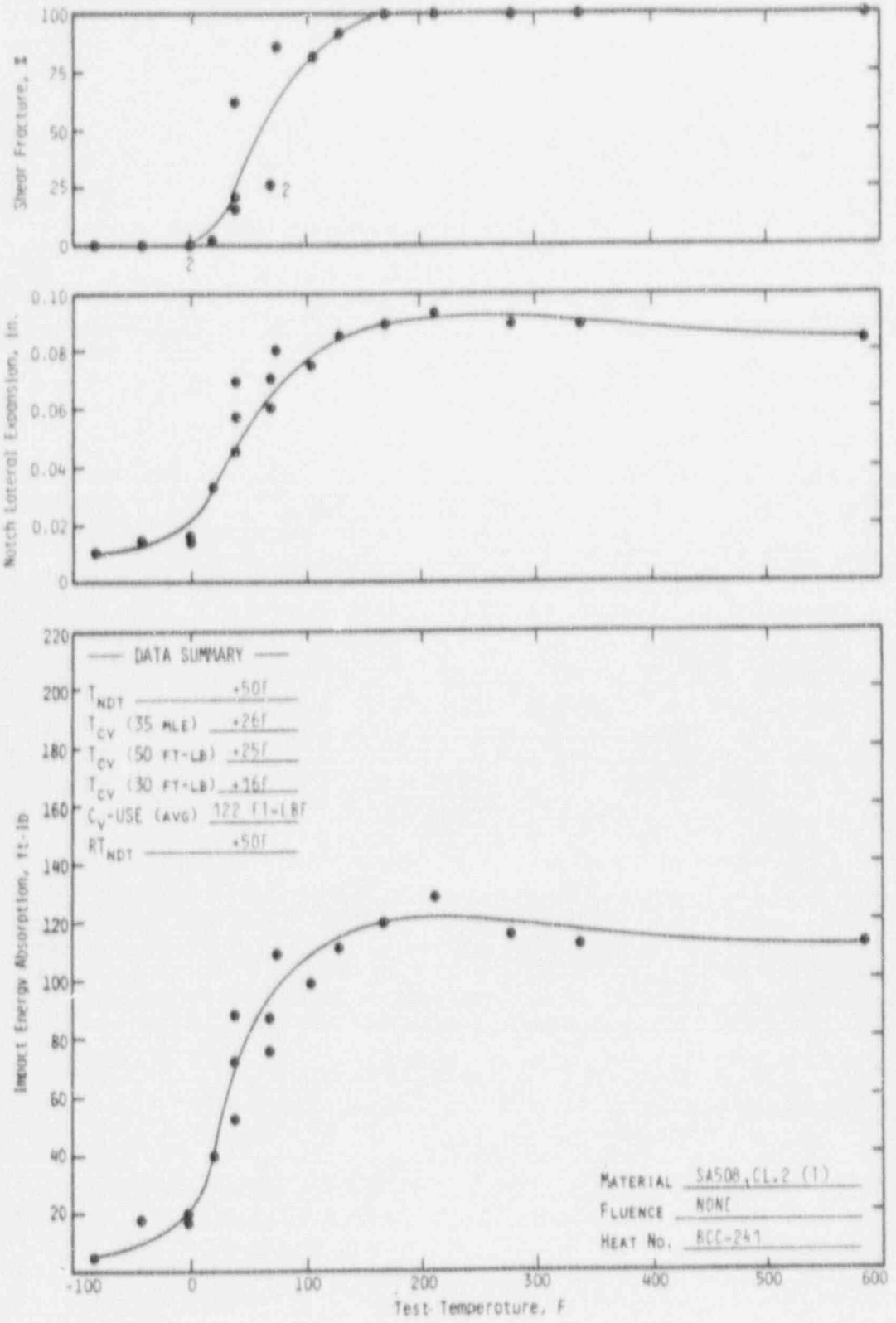

Figure C-2. Impact Data for Unirradiated Shell Forging Material, Heat-Affected Zone, Heat BCC-241

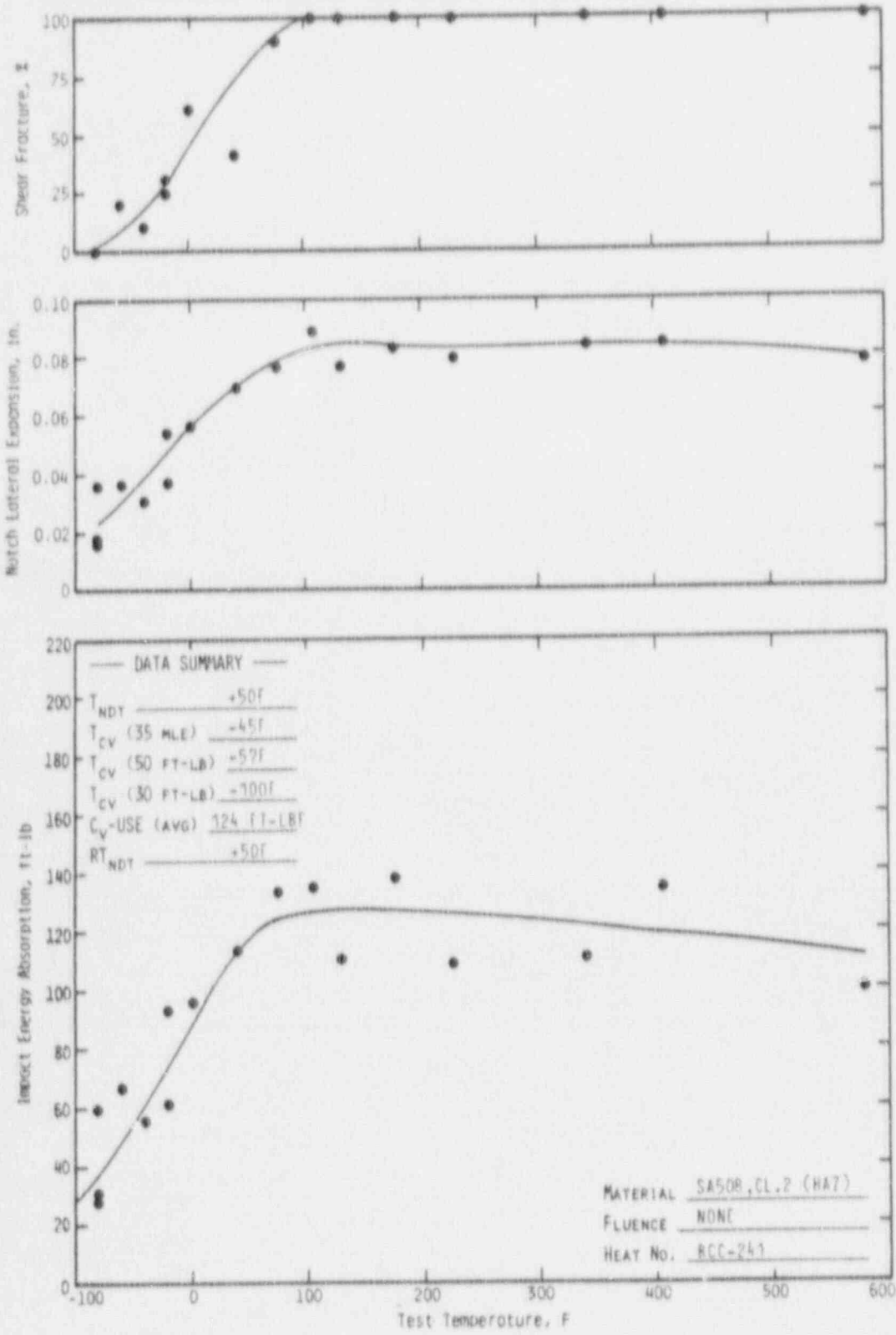

Figure C-3. Impact Data for Unirradiated Weld Metal, WF-182-1

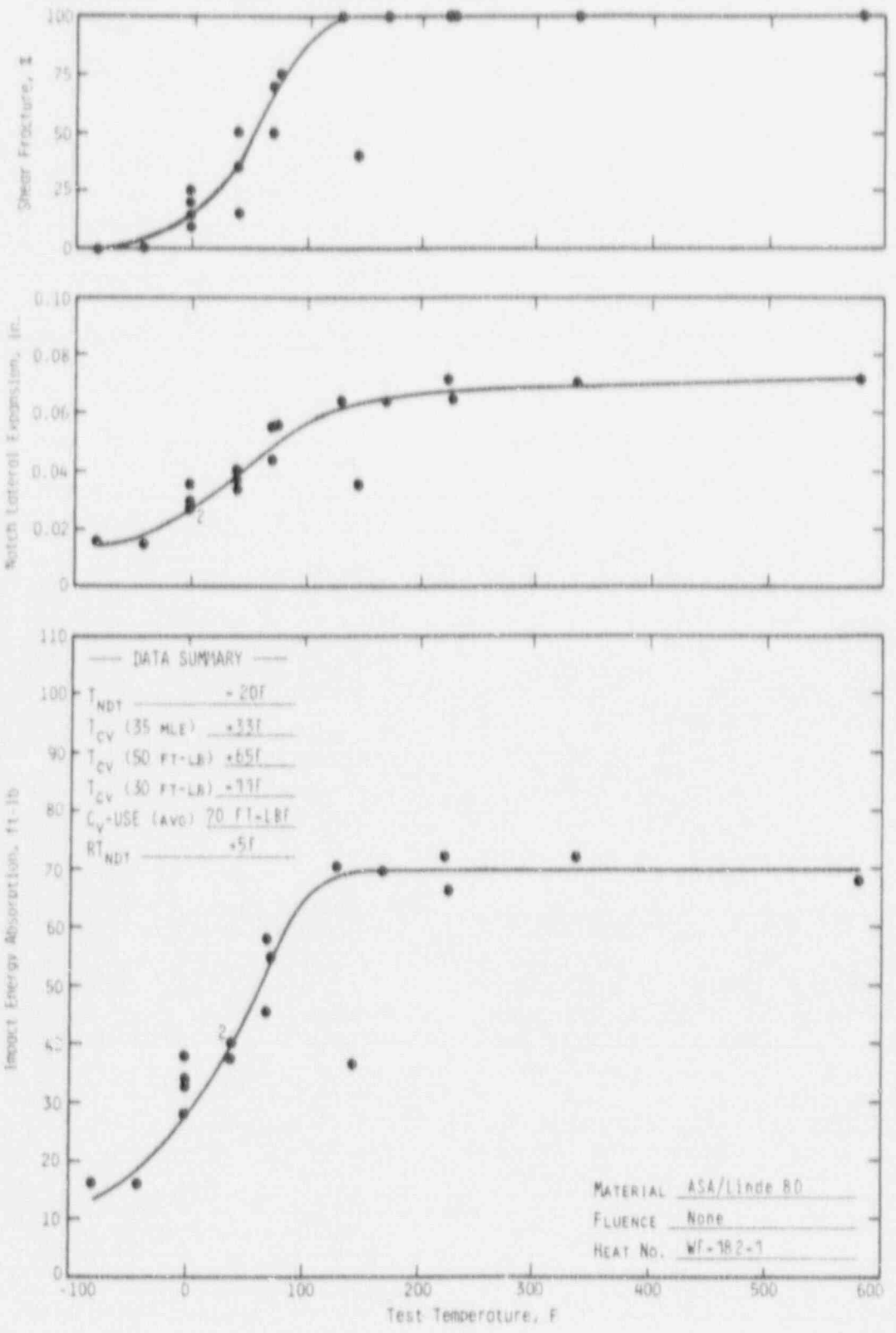

APPENDIX D

Fluence Analysis Methodology

1. Analytical Method

A semiempirical method is used to calculate the capsule and vessel flux. The method employs explicit modeling of the reactor vessel and internals and uses an average core power distribution in the discrete ordinates transport code DOTIV, version 4.3. DOTIV calculates the energy and space dependent neutron flux for the specific reactor under consideration. This semiempirical method is conveniently outlined in Figures D-1 (capsule flux) and D-2 (vessel flux).

The two-dimensional transport code DOTIV was used to calculate the energy- and space-dependent neutron flux at all points of interest in the reactor system. DOTIV uses the discrete ordinates method of solution of the Boltzmann transport equation and has multi-group and asymmetric scattering capability. The reference calculational model is an R-θ geometric representation of a plan view through the reactor core midplane which includes the core, core liner, coolant, core barrel, thermal shield, pressure vessel, and concrete. The material and geometry model, represented in Figure D-3, uses one-eight core symmetry. In order to include reasonable geometric detail within the computer memory limitations, the code parameters are specified as P_3 order of scattering, S_8 quadrature, and 40 energy groups. The P_3 order of scattering adequately describes the predominately forward scattering of neutrons observed in the deep penetration of steel and water media, as demonstrated by the close agreement between measured and calculated dosimeter activities. The S_8 symmetric quadrature has generally produced accurate results in discrete ordinates solutions for similar problems, and is used routinely in the B&W R-θ DOT analyses.

Flux generation in the core was represented by a fixed distributed source which the code derives based on a ^{235}U fission spectrum, the input relative power distribution, and a normalization factor to adjust flux level to the desired power density.

Geometrical Configuration

For modeling purposes, the actual geometrical configuration is divided into three parts, as shown in Figure D-3. The first part, Model "A," is used to generate

the energy-dependent angular flux at the inner boundary of Model "B," which begins at the outer surface of the core barrel. Model A includes a detailed representation of the core baffle (or liner) in R-θ geometry that has been checked for both metal thickness and total metal volume to ensure that the DOT approximation to the actual geometry is as accurate as possible for these two very important parameters. The second, Model B, contains an explicit representation of the surveillance capsule and associated components. The B&W Owners Group's Flux Perturbation Experiment[25] verified that the surveillance capsule must be explicitly included in the DOT models used for capsule and vessel flux calculations in order to obtain the desired accuracy. The magnitude of the perturbations in the fast flux due to the presence of the capsule was determined in the Perturbation Experiment to be as high as 47% at the capsule center and as high as 10% at the inner surface of the reactor vessel. Detailed explicit modeling of the capsule, capsule holder tube, and internal components is therefore incorporated into the DOT calculational models. The third, Model "C," is similar to Model B except that no capsule is included. Model C is used in determining the vessel flux in quadrants that do not contain a surveillance capsule; typically these quadrants contain the azimuthal flux peak on the inside surface of the reactor vessel.

An overlap region of approximately 33.02 cm or 17 radial intervals is specified between Model A and Models B or C. The width of this overlap region, which is fixed by the placement of the Model A vacuum boundary and the Model B boundary source, was determined by an iterative process that resulted in close agreement between the overlap region flux as predicted by Models A and B or C. The outer boundary was placed sufficiently far into the concrete shield (cavity wall) that the use of a "vacuum" boundary condition does not cause a perturbation in the flux at the points of interest.

Macroscopic Cross Sections

Macroscopic cross sections, required for transport analyses, are obtained with the mixing code GIP. Nominal compositions are used for the structural metals. Coolant compositions were determined using the average boron concentration over

a fuel cycle and the bulk temperature of the region. The core region is a homogeneous mixture of fuel, fuel cladding, structure, and coolant.

The cross-section library presently used is the (22-neutron group and 18-gamma group) CASK 23E coupled set. The dosimeter reaction cross sections are based on the ENDF/B5 library, and are listed in Table E-3. The measured and calculated dosimeters activities are compared in Table D-1.

Distributed Source

The neutron population in the core during full power operation is a function of neutron energy, space, and time. The time dependence is accounted for in the analysis by calculating the time-weighted average neutron source, i.e. the neutron source corresponding to the time-weighted average power distribution. The effects of the other two independent variables, energy and space, are accounted for by using a finite but appropriately large number of discrete intervals in energy and space. In each of these intervals the neutron source is assumed to be invariant and independent of all other variables. The space and energy dependent source function can be considered as the product of a discretely expressed "spatial function" and a magnitude coefficient, i.e.

$$Sv_{ijg} = \underbrace{[\nu/K\ P_p]}_{\text{magnitude}} \times \underbrace{[RPD_{ij} X_g]}_{\text{spatial}} \qquad (D\text{-}1)$$

where:

Sv_{ijg} = Energy-and space-dependent neutron source, n/cc-sec,

ν/K = Fission neutron production rate, n/w-sec,

P_p = Average power density in core, w/cc,

RPD_{ij} = Relative power density at interval (i,j), unitless,

X_g = Fission spectrum, fraction of fission neutrons having energy in group "g,"

i = Radial coordinate index,

j = Azimuthal coordinate index,

g = Energy group index.

The spatial dependence of the flux is directly related to the RPD distribution. Evcn though the entire (eighth-core symmetric) RPD distribution is modeled in the analysis, only the peripheral fuel assemblies contribute significantly to the ex-core flux. The axial average pin-by-pin RPD distribution is calculated on a quarter-core symmetric basis for 8 to 12 times during each core cycle for the entire capsule irradiation period. The time-weighted average RPD distribution is used to generate the normalized space and energy dependency of the neutron source. Calculations for the energy and space dependent, time-averaged flux were performed for the midpoint of each DOT interval throughout the model. Since the reference model calculation produced fluxes in the R-θ plane that are averaged over the core height, an axial correction factor was required to adjust these fluxes to the capsule elevation. The factor used (1.14) was prescribed in BAW-1485P.[14]

1.1. Capsule Flux and Fluence Calculation

As discussed above, the DOTIV code was used to explicitly model the capsule assembly and to calculate the neutron flux as a function of energy within the capsule. The calculated fluxes were used in the following equation to obtain calculated activities for comparison with the measured data. The calculated activity for reaction product D_i, in (μCi/gm) is:

$$D_i = \frac{N \quad f_i}{(3.7 \times 10^{4})A_n} \sum_{E} \sigma_n (E)\, \phi (E) \sum_{j} F_j \,(1-e^{-\lambda_i t_j})\, e^{-\lambda_i (T - \tau_j)} \qquad (D\text{-}2)$$

where:

N = Avogadro's number,

A_n = Atomic weight of target material n,

f_i = Either weight fraction of target isotope in n-th material or the fission yield of the desired isotope,

$\sigma_n(E)$ = Group-averaged cross sections for material n (listed in Table E-3)

$\phi(E)$ = Group averaged fluxes calculated by DOTIV analysis,

F_j = Fraction of full power during j-th time interval, t_j

λ_i = Decay constant of the ith isotope,

T = Sum of total irradiation time, i.e., residual time in reactor, and the wait time between reactor shutdown and counting times,

τ_j = Cumulative time from reactor startup to end of j-th time period.

t_j = Length of the j-th time period

Adjustments were made to the calculated dosimeter activities to correct for the effects listed below:

Short half-life adjustments to Ni and Fe dosimeter activities

Photofission adjustments to ^{238}U and ^{237}Np dosimeter activities

Fissile impurity adjustments to ^{238}U dosimeter activities

After making these adjustments the calculated dosimeter activities were used with the corresponding measured activities to obtain the flux normalization factors:

$$C_i = \frac{D_i \text{ (measured)}}{D_i \text{ (calculated)}}.$$

These normalization factors were evaluated, averaged, and then used to adjust the calculated test specimen flux and fluence to be consistent with the dosimeter measurements. Additionally, the normalization factor was used to update the average normalization factor which had been derived from previous analyses. The updated normalization factor was then used to adjust the calculated vessel flux and fluence. The flux normalization factors are given in Table D-1.

2. Vessel Fluence Extrapolation

For past core cycles, fluence values in the pressure vessel are calculated as described above. Extrapolation to future cycles is required to predict the

useful vessel life. Three time periods are considered in the extrapolation: 1) operation to date for which vessel fluence has been calculated, 2) future fuel cycles for which PDQ calculations have been performed, and 3) future cycles for which no analyses exist.

For the Davis Besse Unit 1 analysis, time period 1 is through cycle 6, time period 2 covers cycle 7, and time period 3 covers from the end of cycle 7 through 32 EFPY. The flux and fluence for time period 2 was estimated by calculating the vessel flux using an adjoint-DOT calculational procedure with the appropriate assembly-average power distributions and integrating these values over time period 2. The extrapolation of the fluence through time period 3 was accomplished by assuming that the average flux during period 3 was equal to the average flux for period 2 (cycle 7).

Table D-1. Normalization Factor

	Measured Activity, μCi/g [a]	Calculated Activity, μCi/g [b]	Flux Normalization Factor
$^{54}Fe(n,p)^{54}Mn$	853.73	1152.79	0.89 [c]
$^{58}Ni(n,p)^{58}Co$	1464.39	2001.51	0.93 [d]
$^{238}U(n,f)^{137}Cs$	11.86	10.36	1.14
$^{237}Np(n,f)^{137}Cs$	70.55	61.69	1.15
		Averaged:	1.03 [e]

(a) Average of four dosimeter wires.

(b) Average at four calculated activities.

(c) Average at four ratios (one for each dosimeter wire) corrected by short half-life factor of 1.195.

(c) Average of four ratios (one for each dosimeter wire) corrected by short half-life factor of 1.264.

(d) Average of all four dosimeters was selected as the normalization constant.

Table D-2. Davis Besse Unit 1 Reactor Vessel Fluence by Cycle

Cycles	Incremental Time, EFPY	Cumulative Time, EFPY	Vessel Flux, n/cm^2s	Vessel Fluence, n/cm^2(c)	
				Incremental	Cumulative
1	1.02	1.02	1.61E+10	5.19E+17	5.19E+17
2-6	4.43	5.45	1.38E+10	1.92E+18	2.44E+18
7	1.07	6.52	1.03E+10	3.47E+17	2.79E+18
	1.48	8.00	1.03E+10(a)	4.80E+17(b)	3.27E+18(b)
	7.00	15.00	1.03E+10(a)	2.28E+18(b)	5.55E+18(b)
	6.00	21.00	1.03E+10(a)	1.95E+18(b)	7.50E+18(b)
	11.00	32.00	1.03E+10(a)	3.60E+18(b)	1.11E+19(b)

(a) Maximum neutron flux at inside surface of reactor vessel, based on fuel cycle designs for future cycle 7, used for extrapolation of fluence to future times.

(b) Extrapolated values.

(c) Peak fluence at inside surface of reactor vessel.

Figure D-1. Rationale for the Calculation of Dosimeter Activities and Neutron Flux in the Capsule

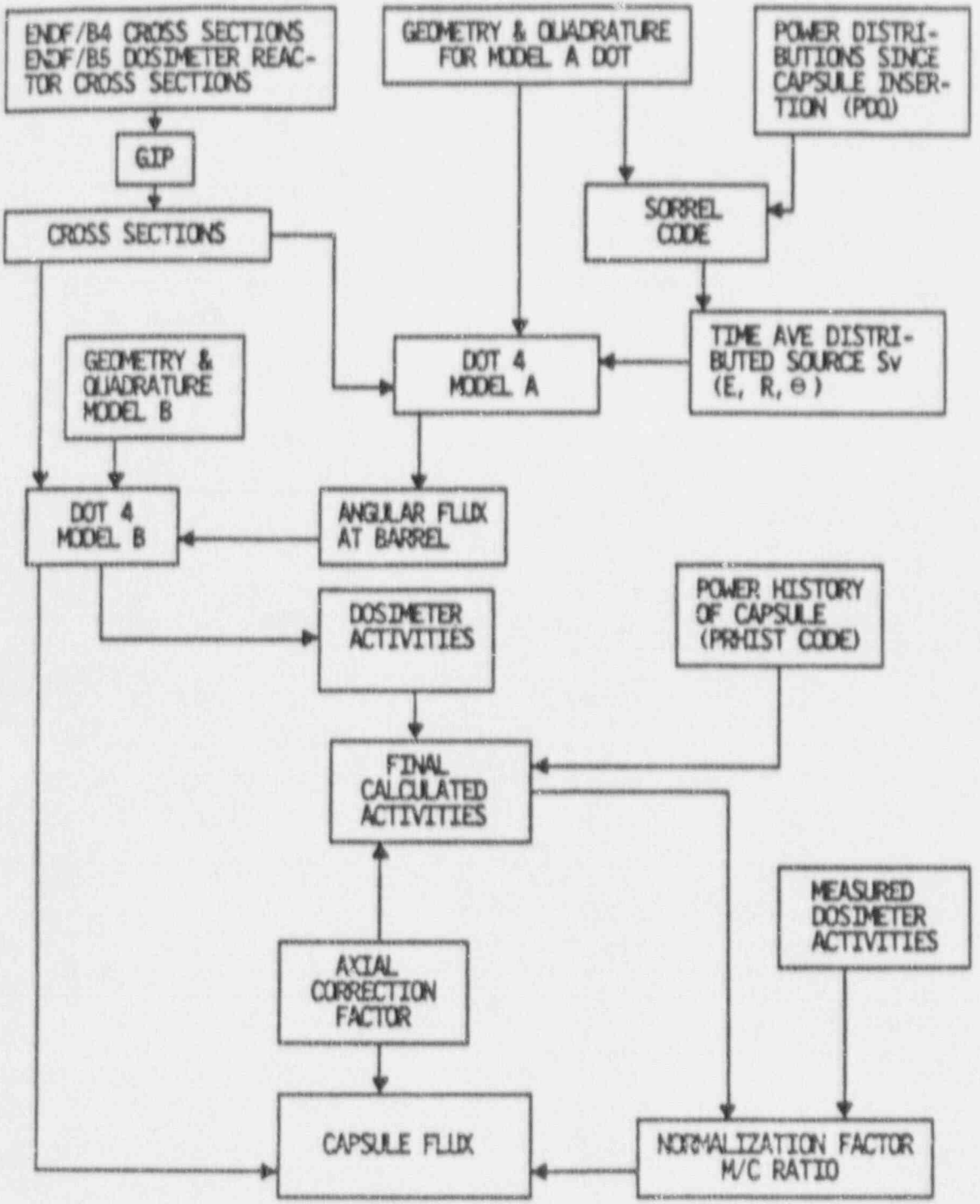

Figure D-2. Rationale for the Calculation of Neutron Flux in the Reactor Vessel

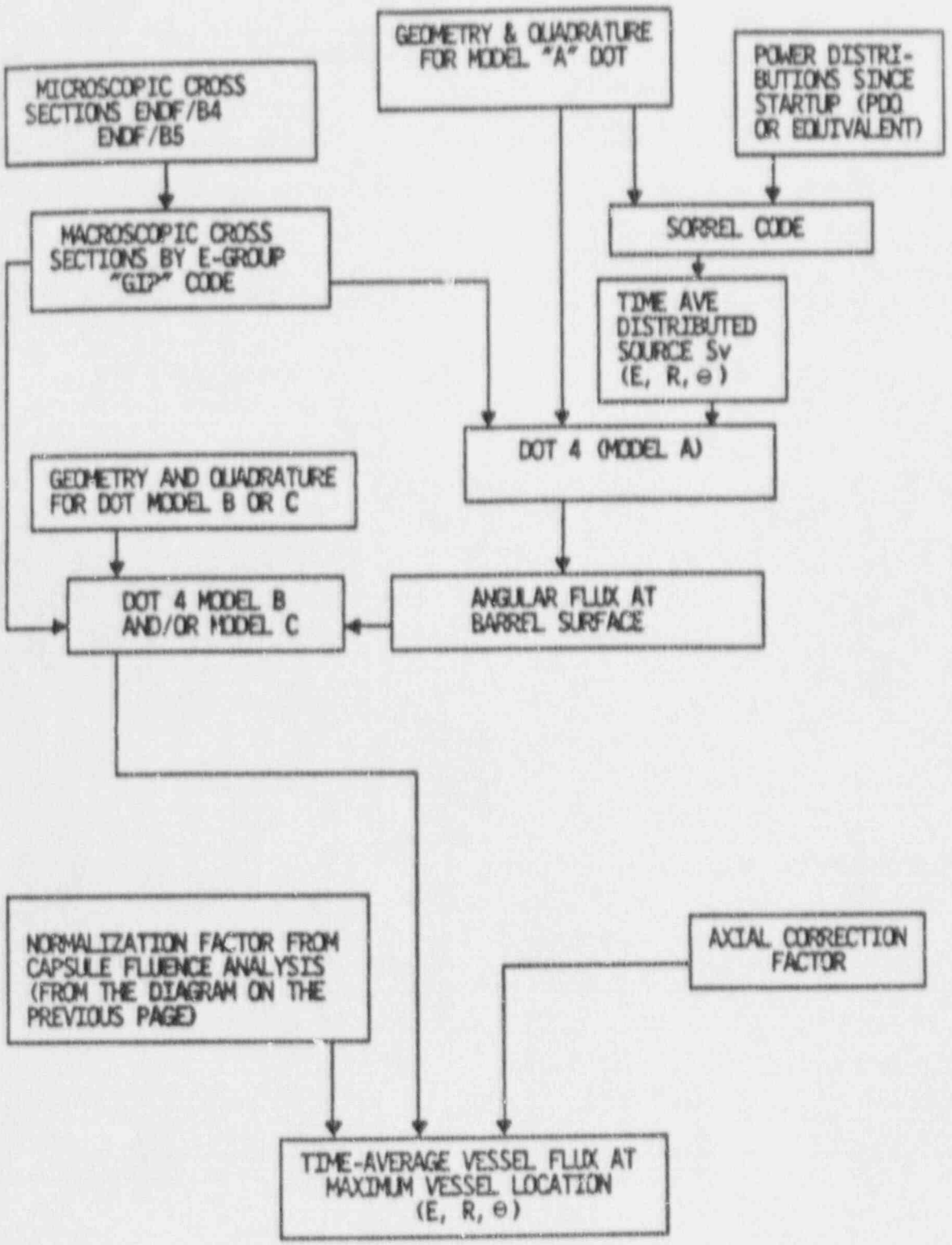

Figure D-3. Plan View Through Reactor Core Midplane
(Reference R-θ Calculation Model)

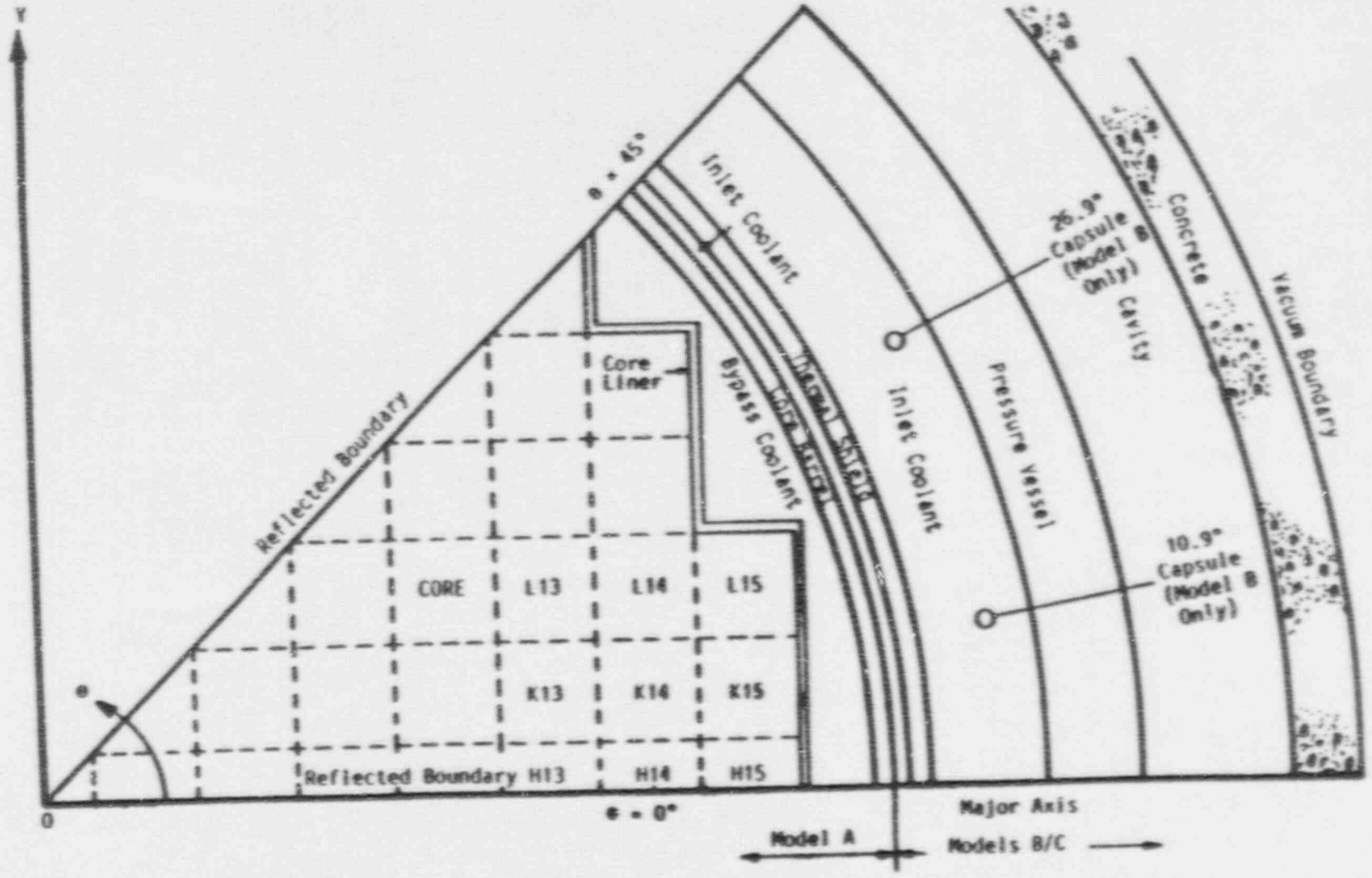

APPENDIX E

Capsule Dosimetry Data

Table E-1 lists the characteristics of the neutron dosimeters. Table E-2 shows the measured activity per gram of target material (i.e., per gram of uranium, nickel, etc.) for the capsule dosimeters. Activation cross sections for the various materials were flux-weighted with the ^{235}U fission spectrum shown in Table E-3.

Table E-1. Detector Composition and Shielding

Detector Material	% Target	Shielding	Reaction
U-Al	10.38% ^{238}U	Cd-Ag	$^{238}U(n,f)^{137}Cs$
Np-Al	1.44% ^{237}Np	Cd-Ag	$^{237}Np(n,f)^{137}Cs$
Ni	67.77% ^{58}Ni	Cd-Ag	$^{58}Ni(n,p)^{58}Co$
Co-Al	0.66% ^{59}Co	Cd	$^{59}Co(n,\gamma)^{60}Co$
Co-Al	0.66% ^{59}Co	None	$^{59}Co(n,\gamma)^{60}Co$
Fe	5.82% ^{54}Fe	None	$^{54}Fe(n,p)^{54}Mn$

Table E-2. Measured Specific Activities (Unadjusted) for Dosimeters in Capsule TE1-D

Detector Material	Dosimeter Reaction	Dosimeter Activity, (μCi/gm of Target) DD1	DD2	DD3	DD4
Ni	$^{58}Ni(n,p)^{58}Co$	1507.23	1433.60	1071.19	1845.52
Fe	$^{54}Fe(n,p)^{54}Mn$	878.81	852.94	627.96	1055.20
U-Al	$^{238}U(n,f)^{137}Cs$	13.80	12.41	9.26	16.97
Np-Al	$^{237}Np(n,f)^{137}Cs$	73.37	64.10	57.95	92.54

Table E-3. Dosimeter Activation Cross Sections, b/atom(a)

G	Energy Range, MeV	$^{237}Np(n,f)$	$^{238}U(n,f)$	$^{58}Ni(n,p)$	$^{54}Fe(n,p)$
1	12.2 - 15	2.323	1.051E+0	4.830E-1	4.133E-1
2	10.0 - 12.2	2.341	9.851E-1	5.735E-1	4.728E-1
3	8.18 - 10.0	2.309	9.935E-1	5.981E-1	4.772E-1
4	6.36 - 8.18	2.093	9.110E-1	5.921E-1	4.714E-1
5	4.96 - 6.36	1.542	5.777E-1	5.223E-1	4.321E-1
6	4.06 - 4.96	1.532	5.454E-1	4.146E-1	3.275E-1
7	3.01 - 4.06	1.614	5.340E-1	2.701E-1	2.193E-1
8	2.46 - 3.01	1.689	5.325E-1	1.445E-1	1.080E-1
9	2.35 - 2.46	1.695	5.399E-1	9.154E-2	5.613E-2
10	1.83 - 2.35	1.676	5.323E-1	4.856E-2	2.940E-2
11	1.11 - 1.83	1.596	2.608E-1	1.180E-2	2.948E-3
12	0.55 - 1.11	1.241	9.845E-3	1.336E-3	6.999E-5
13	0.111 - 0.55	2.352E-1	2.436E-4	5.013E-4	6.419E-8
14	0.0033 - 0.111	1.200E-2	6.818E-5	1.512E-5	0

(a) ENDF/B5 values that have been flux weighted (over CASK energy groups) based on a ^{235}U fission spectrum in the fast energy range plus a 1/E shape in the intermediate energy range.

APPENDIX F

References

1. A. L. Lowe, Jr., et al., Analysis of Capsule TE1-F from Toledo Edison Company, Davis-Besse Nuclear Power Station, Unit 1, Reactor Vessel Materials Surveillance Program, BAW-1701, Babcock & Wilcox, Lynchburg, Virginia, January 1982.

2. A. L. Lowe, Jr., et al., Analysis of Capsule TE1-B from Toledo Edison Company, Davis-Besse Nuclear Power Station, Unit 1, Reactor Vessel Materials Surveillance Program, BAW-1834, Babcock & Wilcox, Lynchburg, Virginia, May 1984.

3. A. L. Lowe, Jr., et al., Analysis of Capsule TE1-A from Toledo Edison Company, Davis-Besse Nuclear Power Station, Unit 1, Reactor Vessel Materials Surveillance Program, BAW-1882, Babcock & Wilcox, Lynchburg, Virginia, September 1985.

4. H. S. Palme, G. S. Carter, and C. L. Whitmarsh, Reactor Vessel Material Surveillance Program -- Compliance With 10CFR50 Appendix H, for Oconee-Class Reactors, BAW-10100A, Babcock & Wilcox, Lynchburg, Virginia, February 1975.

5. Code of Federal Regulation, Title 10, Part 50, Fracture Toughness Requirements for Light-Water Nuclear Power Reactors, Appendix H, Reactor Vessel Material Surveillance Program Requirements.

6. American Society for Testing and Materials, Standard Recommended Practice for Surveillance Tests for Nuclear Reactor Vessels, E185-73, March 1, 1973.

7. S. Fyfitch, L. B. Gross, and A. L. Lowe, Jr., Master Integrated Reactor Vessel Surveillance Program, BAW-1543, Rev. 3, Babcock & Wilcox, Lynchburg, Virginia, September 1989.

8. American Society for Testing and Materials, Standard Practice for Conducting Surveillance Tests for Light Water Cooled Nuclear Power Reactor Vessels, E185-82, July 1, 1982.

9. Code of Federal Regulation, Title 10, Part 50, Fracture Toughness Requirements for Light-Water Nuclear Power Reactors, Appendix G, Fracture Toughness Requirements.

10. K. E. Moore and A. S. Heller, Chemistry of 177-FA B&W Owners' Group Reactor Vessel Beltline Welds, BAW-1500P, Babcock & Wilcox, Lynchburg, Virginia, September 1978.

11. American Society for Testing and Materials, Methods and Definitions for Mechanical Testing of Steel Products, A370-77, June 24, 1977.

12. American Society for Testing and Materials, Methods for Notched Bar Impact Testing of Metallic Materials, E23-82, March 5, 1982.

13. A. L. Lowe, Jr., et al, Evaluation of Surveillance Capsule Temperatures, BAW-2040, Babcock & Wilcox, Lynchburg, Virginia, March 1989.

14. A. L. Lowe, Jr., et al, Fracture Toughness Test Results from Capsule TE1-D, The Toledo Edison Company Davis Besse Nuclear Power Station Unit 1 Reactor Vessel Material Surveillance Program, BAW-2128, B&W Nuclear Service Company, Lynchburg, Virginia, To be Published.

15. S. Q. King, Pressure Vessel Fluence Analysis for 177-FA Reactors, BAW-1485P, Revision 1, Babcock & Wilcox, Lynchburg, Va., April 1988.

16. B&W's Version of DOTIV Version 4.3, One- and Two-Dimensional Transport Code System," Oak Ridge National Laboratory, Distributed by the Radiation Shielding Information Center as CC-429, November 1, 1983.

17. "CASK-40-Group Coupled Neutron and Gamma-Ray Cross Section Data," Radiation Shielding Information Center, DLC-23E.

18. Dosimeter File ENDF/B5 Tape 531, distributed March 1984, National Neutron Data Center, Brookhaven National Laboratory, Upton, Long Island, NY.

19. American Society of Testing Materials, Characterizing Neutron Exposures in Ferritic Steels in Terms of Displacements Per Atom (DPA), E693-79 (Reapproved 1985).

20. U.S. Nuclear Regulatory Commission, Radiation Damage to Reactor Vessel Material, Regulatory Guide 1.99, Revision 2, May 1988.

21. A. S. Heller and A. L. Lowe, Jr., Correlations for Predicting the Effects of Neutron Radiation on Linde 80 Submerged-Arc Welds, BAW-1803, Babcock & Wilcox, Lynchburg, Virginia, January 1984.

22. The Third Surveillance Test on The Ko-Ri Unit No. 1 Reactor Vessel Materials (Capsule S), June 1986.

23. J. D. Aadland, Babcock & Wilcox Owner's Group 177-Fuel Assembly Reactor Vessel and Surveillance Program Materials Information, BAW-1820, Babcock & Wilcox, Lynchburg, Virginia, December 1984.

24. K. E. Moore and A. S. Heller, B&W 177-FA Reactor Vessel Beltline Weld Chemistry Study, BAW-1799, Babcock & Wilcox, Lynchburg, Virginia, July 1983.

25. N. L. Snider and L. A. Hassler, B&WOG Flux Perturbation Experiment at ORNL, Measured and Calculated Dosimeter Results, BAW-1886, Babcock & Wilcox, Lynchburg, Virginia, September 1985.